A new species of the tetralophodont amebelodontine *Konobelodon* Lambert, 1990 (Proboscidea, Mammalia) from the Late Miocene of China

ShiQi WANG
Key Laboratory of Vertebrate Evolution and Human Origins of the Chinese Academy of Sciences,
Institute of Vertebrate Paleontology and Paleoanthropology,
Chinese Academy of Sciences, no. 142 Xizhimenwai Street, 100044 Beijing (China)
and CAS Center for Excellence in Tibetan Plateau Earth Sciences,
no. 16 Lincui Street, 100101 Beijing (China)
and Key Laboratory of Economic Stratigraphy and Palaeogeography,
Chinese Academy of Sciences (Nanjing Institute of Geology and Palaeontology),
no. 39 Beijingdong Street, 210008 Nanjing (China)
wangshiqi@ivpp.ac.cn

QinQin SHI
Key Laboratory of Vertebrate Evolution and Human Origins of the Chinese Academy of Sciences,
Institute of Vertebrate Paleontology and Paleoanthropology, Chinese Academy of Sciences,
no. 142 Xizhimenwai Street, 100044 Beijing (China)
shiqinqin@ivpp.ac.cn

Wen HE
ShanQin CHEN
Hezheng Paleozoological Museum,
Liangjiazhuang, 731200 Hezheng (China)
hzbwg_5524668@126.com
hzbwg_chenshanqin@126.com

XiangWen YANG
Key Laboratory of Vertebrate Evolution and Human Origins of the Chinese Academy of Sciences,
Institute of Vertebrate Paleontology and Paleoanthropology, Chinese Academy of Sciences,
no. 142 Xizhimenwai Street, 100044 Beijing (China)
and University of the Chinese Academy of Sciences
no.19A Yuquan Road, 100049 Beijing (China)
344490433@qq.com

Published on 25 March 2016

urn:lsid:zoobank.org:pub:AD9C6BAE-8A37-4201-BFA6-C49739CFDD60

Wang S., Shi Q., He W., Chen S. & Yang X. 2016. — A new species of the tetralophodont amebelodontine *Konobelodon* Lambert, 1990 (Proboscidea, Mammalia) from the Late Miocene of China. *Geodiversitas* 38 (1): 65-97. http://dx.doi.org/10.5252/g2016n1a4

KEY WORDS
Amebelodontinae,
Konobelodon,
tetralophodont
gomphotheres,
Late Miocene,
China,
new species.

ABSTRACT
Here we describe a new species of *Konobelodon* Lambert, 1990 – a poorly known tetralophodont shovel-tusked proboscidean – from the Late Miocene of the Linxia Basin, China. Detailed osteological anatomies of skulls, teeth, and partial postcranial bones of the new taxon, *Konobelodon robustus* n. sp., are described and detailed morphological comparisons with the other species of *Konobelodon* (*K. atticus* (Wagner, 1857) = *Mastodon grandincisivus,* Schlesinger 1917, and *K. britti* (Lambert, 1990)) and

other gomphotheres are conducted. The skull and jaw-closing muscles of a juvenile individual of the new species are reconstructed and the body mass is estimated based on its limb bones. Phylogenetic analysis of genera within Elephantimorpha results in three most parsimonious trees, of which two support a sister-group relationship between *Konobelodon* and *Platybelodon*, within a monophyletic Amebelodontinae. The new results enhance our knowledge on the anatomy and phylogeny of *Konobelodon*, and indicate pronounced diversification and strong parallel evolution in the amebelodontines.

RÉSUMÉ

Une nouvelle espèce de l'amébélodontiné tétralophodonte Konobelodon *Lambert, 1990 (Proboscidea, Mammalia) du Miocène supérieur de Chine.*

Nous décrivons ici une nouvelle espèce de *Konobelodon* Lambert, 1990 – un amébélodontiné tétralophodonte peu connu parmi les proboscidiens – du Miocène supérieur du Bassin de Linxia, Chine. L'anatomie ostéologique détaillée des crânes, des dents et d'une partie des os postcrâniens du nouveau taxon, *Konobelodon robustus* n. sp., est décrite. Des comparaisons morphologiques détaillées avec les autres espèces de *Konobelodon* (*K. atticus* (Wagner, 1857) = *Mastodon grandincisivus* Schlesinger, 1917*,* et *K. britti* (Lambert, 1990)) et d'autres gomphothères sont effectuées. Le crâne et les muscles de la mastication d'un individu juvénile de *Konobelodon robustus* n. sp. sont reconstruits et le poids du corps est estimé sur la base des os de ses membres. L'analyse phylogénétique des genres d'Elephantimorpha donne trois arbres parmi les plus parcimonieux. Deux suggèrent que *Konobelodon* et *Platybelodon* sont groupe-frère au sein d'un groupe monophylétique d'Amebelodontinae. Ces nouveaux résultats précisent nos connaissances sur l'anatomie et sur la phylogénie des *Konobelodon*. Ils indiquent aussi une diversification rapide et une forte évolution parallèle chez les amébélodontinés.

MOTS CLÉS
Amebelodontinae,
Konobelodon,
Gomphothères
tetralophodonte,
Miocène supérieur,
Chine,
espèce nouvelle.

INTRODUCTION

Schlesinger (1917) established "*Mastodon* (*Bunolophodon*) *grandincisivum*" Schlesinger, 1917 based on a fragmentary lower tusk from Maragheh, Iran, and three isolated molars from Mannersdorf bei Angern, Austria. He also considered the previously reported *M.* cf. *longirostris* Kaup, 1832 from Kertch (now in Crimea) (Pavlow 1903) to be the same taxon. Shortly afterwards, Schlesinger (1922) reported an incomplete skeleton of "*M. grandincisivus*" from Pestszentlőrincz, Hungary. As the genus "*Mastodon*" Cuvier, 1817 was confined to the Pleistocene-aged "true" American mastodon (nowadays synonymized with *Mammut americanum* (Kerr, 1792)), later Osborn (1936) transferred "*M. grandincisivus*" to *Tetralophodon* Falconer, 1857. This opinion has been followed by subsequent researchers (e.g., Bakalov & Nikolov 1962; Gaziry 1976). But because the strong and flattened lower tusks are markedly distinct from *Tetralophodon longirostris* Kaup, 1832 (the type species), which possesses relatively reduced and sub-circular lower tusks, Tobien (1978) considered "*M. grandincisivus*" to be a species of *Stegotetrabelodon* Petrocchi, 1941 based on the elongated mandibular symphysis and lower tusks in both taxa. This viewpoint considers "*M. grandincisivus*" to be the ancestor of the true elephants, and has been followed by some researchers (e.g., Madden 1982; Chow & Zhang 1983; Gaziry 1987; Tobien *et al.* 1988; Kovachev 2004). The systematic results of Tassy & Darlu (1986, 1987), Kalb *et al.* (1996) and Ferretti *et al.* (2003) showed that "*M. grandincisivus*" does not cluster with *Stegotetrabelodon*. Tassy (1983a, 1985, 1986, 1999) considered the taxon to be an amebelodontine because of the morphology of the mandible and the lower tusks. This view was followed by subsequent researchers (Markov 2004, 2008; Geraads *et al.* 2005; Konidaris *et al.* 2014). Markov (2008) summarized its occurrences in western Asia, eastern Europe, northern Africa, and possibly southern Asia in the Late Miocene, while Markov *et al.* (2014) described new anatomic information based on a juvenile mandible from Hadzhidimovo, Bulgaria. Recently, Konidaris *et al.* (2014) synonymized "*M. grandincisivus*" with "*Tetralophodon atticus*" (Wagner, 1857) based on a revision of fossil proboscideans from Pikermi, Greece, and proposed that the Pikermi tetralophodonts belong to the tetralophodont amebelodontine *Konobelodon* Lambert, 1990. Konidaris *et al.* (2014) suggested that all the Turolian (MN 11-MN 13) tetralophodont amebelodontines from western Eurasia should be attributed to *Konobelodon atticus*, which has nomenclatural priority over "*grandincisivus*".

Konobelodon was originally established as a subgenus of *Amebelodon*, differing from the other members of *Amebelodon* (*Amebelodon*) in the presence of the tubular structure in the lower tusks and the tetralophodont molars (Lambert 1990). Initially, the type and the only species of *Konobelodon* was *K. britti* (Lambert, 1990); no cranium and complete mandible of *K. britti* have yet been reported. In the traditional view, the subfamily Amebelodontinae is subdivided into two groups. One includes *Archaeobelodon* Tassy, 1984, *Serbelodon* Frick, 1933, *Protanancus* Arambourg, 1945, *Amebelodon* Barbour, 1927, *Progomphotherium* Pickford, 2003, and *Afromastodon*

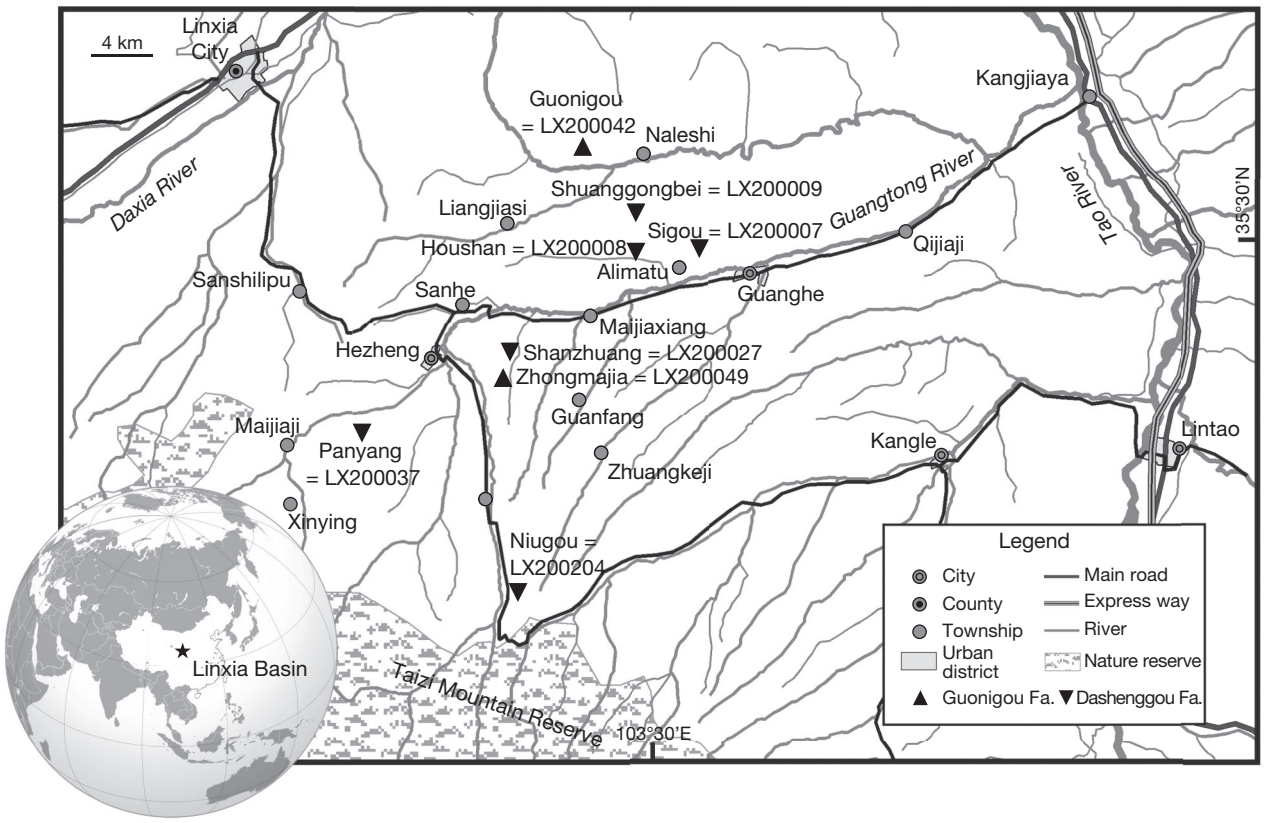

FIG. 1. — Fossil sites yielding *Konobelodon robustus* n. sp. in the Linxia Basin (China). The globe was taken from www.wikipedia.com.

Pickford, 2003 with concentric laminated dentine in the lower tusks; the other includes *Platybelodon* Borissiak, 1928 and *Torynobelodon* Barbour, 1929, with tubular structure in the lower tusks (Tassy 1986; Sanders *et al.* 2010). Thus, *Konobelodon* appears to belong to the latter group. As *K. robustus* n. sp. from the Linxia Basin is represented by more complete material than *K. britti* and *K. atticus*, further study of this material is helpful for understanding the evolution and differentiation of the genus *Konobelodon* and the subfamily Amebelodontinae.

Abundant tetralophodont remains were discovered in 1980s, in the Linxia Basin of northern China (Fig. 1), including complete crania, mandibles, and some postcranial bones. The material was previously identified as *Tetralophodon* sp. and *T. exoletus* Hopwood, 1935 (Deng *et al.* 2004, 2013; Deng 2006a). However, without exception, all the mandibles of these remains possess an elongated mandibular symphysis and flattened lower tusks. This feature combination groups the Linxia specimens with "*M. grandincisivus*" rather than with *Tetralophodon* (Wang *et al.* 2013a). In this paper, following the opinion of Konidaris *et al.* (2014), we attribute the Linxia material and "*M. grandincisivus*" to *Konobelodon*, and establish a new species *K. robustus* n. sp., for the Linxia material. Detailed comparisons of the new taxon with the members of Amebelodontinae, Stegotetrabelodontinae, and other tetralophodont gomphotheres will also be performed. We believe that this study is a contribution towards resolving the century-old problem of "*M. grandincisivus*".

GEOLOGICAL SETTINGS

Neogene sediments are well developed in the Linxia Basin, especially the Late Miocene deposits (Fig. 2). Based on Deng *et al.* (2013), fossils from the Late Miocene Liushu Formation of the Linxia Basin were subdivided into four faunal communities: the Guonigou, Dashenggou, Yangjiashan, and Qingbushan faunas (from earliest to latest). The first two faunas, Guonigou and Dashenggou, correspond to the European Vallesian and the later two to the Turolian (Fig. 1). All the remains of *K. robustus* n. sp. were discovered from eight sites belonging to the Vallesian Guonigou and Dashenggou faunas. Two sites, LX200049 (= Zhongmajia) and LX200042 (= Guonigou) (Fig. 1), correspond to the Guonigou Fauna. This fauna includes *Pararhizomys hipparionum* Teilhard & Young, 1931, *Gobicyon* sp., *Dinocrocuta gigantea* (Schlosser, 1903), *Machairodus palanderi* Zdansky, 1924, *Prodeinotherium sinense* Qiu, Wang, Li, Deng & Sun, 2007, *Hipparion dongxiangense* Qiu & Xie, 1998, *H. weihoense* Liu, Li & Zhai, 1978, *Chilotherium* sp., *C. primigenius* Deng, 2006, *Parelasmotherium simply* (Chow, 1958), *P. linxiaense* Deng, 2001, *Ningxiatherium euryrhinus* Deng, 2008, *Listriodon mongoliensis* Colbert, 1934, *Shaanxispira* sp. and *Tsaidamotherium brevirostrum* Shi, 2014 (Deng *et al.* 2013; Shi 2014). The site LX200042 occurs just slightly higher than the Middle/Late Miocene boundary, and yields the most primitive Chinese hipparionines, *Hipparion dongxiangense* (Qiu & Xie 1998). The site LX200049 yields the

most primitive chilothere, *Chilotherium primigenius* (Deng 2006b). Thus, this fauna represents the earliest Late Miocene (Deng *et al.* 2013), corresponding to MN 9 or NMU 8. The other six sites, LX200027 (= Shanzhuang), LX200009 (= Shuanggongbei), LX200204 (= Niugou), LX200037 (= Panyang), LX200007 (= Sigou), LX200008 (= Houshan) (Fig. 1) correspond to the Dashenggou Fauna. This fauna includes *Prosiphneus* sp., *Pararhizomys hipparionum*, *Agriotherium* sp., *Indarctos* sp., *Sinictis* sp., *Parataxidea sinensis* Zdansky, 1924, *Melodon majori* Zdansky, 1924, *Promephitis parvus* Wang & Qiu, 2004, *P. hootoni* Senyürek, 1954, *Ictitherium* sp., *Hyaenictitherium wongii* (Zdansky, 1924), *H. hyaenoides* (Zdansky, 1924), *Dinocrocuta gigantea*, *Machairodus palanderi*, *Felis* sp., *Hipparion chiai* Liu, Li & Zhai, 1978, *H. weihoense*, *H. dermatorhinum* Sefve, 1927, *Chalicotherium* sp., *Acerorhinus hezhengensis* Qiu, Xie & Yan, 1987, *Chilotherium wimani* Ringström, 1924, *Iranotherium morgani* (Mequenem, 1908), *Diceros gansuensis* Deng, 2007, *Chleuastochoerus stehlini* (Schlosser, 1903), *Metacervulus* sp., *Samotherium* sp., *Honanotherium schlosseri* Bohlin, 1927, *Shaanxispira linxiaensis* Shi, He & Chen, 2014, *Gazella* sp., *Miotragocerus* sp., *Hezhengia bohlini* Qiu, Wang & Xie, 2000 and *Megahezhengia longicornis* Shi, 2012 (Shi 2012; Deng *et al.* 2013; Shi *et al.* 2014). This fauna corresponds to MN 10 or NMU 9.

MATERIAL AND METHODS

Material

The new material that we describe herein is housed in the collections of the HMV and the IVPP, and includes crania, mandibles, isolated teeth, and postcranial bones. For comparative study, data regarding *Konobelodon atticus* and *Tetralophodon longirostris* are from the NHMW material. Data on *Platybelodon grangeri* (Osborn, 1929) are from the collections of the HMV and the AMNH. Data on *Gomphotherium angustidens* (Cuvier, 1817) and the *Archaeobelodon filholi* (Frick, 1933) are from the MNHN. Other data are from previous publications.

Methods

Measurements

Cranial and mandibular measurements follow Tassy (2013), and postcranial measurements follow Göhlich (1998). All measurements were taken using callipers.

Nomenclature

The terminology of the occlusal structures of gomphotheriid cheek teeth follows Tassy (2014), that of the cranial and postcranial skeleton mainly follows Ferretti (2010), and partial terms are from Sisson (1953). Dental age determination of crania and mandibles is based on the method introduced by Tassy (2013) for trilophodont gomphotheres. Although the study material is a tetralophodont gomphothere, we only consider the wear pattern of the first three loph(id)s. We found that our material matches the Tassy's dental age scale well.

Cladistic analysis

A cladistic analysis was performed to investigate the phylogenetic interrelationships of our new taxon with several representatives of Elephantiformes. In the present analysis, in addition to our new species we chose 16 other genera, including *Phiomia* Andrews & Beadnell, 1902, *Zygolophodon* Vacek, 1877, *Choerolophodon* Schlesinger, 1917, *Archaeobelodon*, *Serbelodon*, *Protanancus*, *Amebelodon*, *Platybelodon*, *Konobelodon*, *Gomphotherium* Burmeister, 1837, *Stegolophodon* Schlesinger, 1917, *Tetralophodon*, *Paratetralophodon* Tassy, 1983, *Anancus* Aymàrd, 1855, *Stegotetrabelodon*, and *Elephas* Linnaeus, 1758. The characters are polarized with respect to *Phiomia* as the outgroup. All characters are treated as unordered (see Appendices 1 and 2). Here we temporarily excluded the African genera *Progomphotherium* and *Afromastodon*; although they were often grouped with amebelodontines (Sanders *et al.* 2010), the incomplete nature of known material hinders for further studying their taxonomy. Characters 5-9, 12, 16, 25, 28, 34-37, and 40 in particular were included because they sampled morphological variations among the gomphothere taxa examined in this study. The remaining characters were chosen based on their previously suggested importance in gomphotheriid and elephantid phylogenetics (Shoshani 1996; Tassy 1996; Prado & Alberdi 2008). Cladograms were obtained from a parsimony analysis carried out using the TNT1.1 program (Goloboff *et al.* 2003). The reported results were based on MPTs and the 50% majority rule tree. Node supports in the 50% majority rule tree were calculated from a bootstrap analysis (1000 replicates).

Abbreviations

AMNH	American Museum of Natural History, New York;
HMV	Hezheng Paleozoological Museum, Hezheng;
IVPP	Institute of Vertebrate Paleontology and Paleoanthropology, Beijing;
MNHN	Muséum national d'Histoire naturelle, Paris;
NHMW	Naturhistorisches Museum Wien, Vienna;
MN	European Neogene mammal zone;
NMU	Chinese Neogene Mammal Faunal Unit;
MPT	most parsimonious tree.

SYSTEMATIC PALAEONTOLOGY

Order PROBOSCIDEA Illiger, 1811
Family GOMPHOTHERIIDAE Hay, 1922
Subfamily AMEBELODONTINAE Barbour, 1927

Genus *Konobelodon* Lambert, 1990

TYPE SPECIES. — *Konobelodon britti* (Lambert, 1990).

DIAGNOSIS. — See Konidaris *et al.* 2014: 1441.

REFERRED SPECIES. — *Konobelodon atticus* (Wagner, 1857).

Konobelodon robustus n. sp.
(Figures 3-12; Tables 1-14)

Tetralophodon sp. – Deng *et al.* 2004: 11; 2013: 256, 257. — Deng 2006: 153.

Tetralophodon exoletus – Deng *et al.* 2004: 11; 2013: 257, 258.

HOLOTYPE. — HMV 0004, an incomplete adult mandible with m3s, dental age XXIII (Fig. 3), loc. LX200049.

PARATYPES. — HMV 0011, almost complete sub-adult mandible with p4 and m1, dental age XII; HMV 1909, almost complete juvenile mandible with both dp2s, dp3s, and dp4s, dental age V; HMV 1910, nearly complete juvenile cranium with both DP2s, DP3s, and DP4s, dental age IV, possibly to be the same individual as HMV 1909, loc. of the above, LX200027; HMV 1904, fragmentary cranium with both DP3s, DP4s, dental age VII, loc. LX200009.

ETYMOLOGY. — *Robustus*, stout or thick, from the robust limb bones in the taxon.

REFERRED MATERIAL. — Loc. **LX200049**: HMV 0003, mandible with both dp3s and dp4s, dental age VII. — Loc. **LX200042**: HMV 1888, left dentary with dp4 and p3, dental age VIII; HMV 1889, left palate with DP2, DP3, and DP4, dental age III; HMV 1861, fragmentary left lower tusk. — Loc. **LX200027**: HMV 0001, mandible with both m2s, dental age XVI, however, two DP3s were incorrectly fixed on the alveoli of m1; HMV 1883, left femur; HMV 1882, left humerus; HMV 1886, left ulna; HMV 1908, mandible with both dp2s and dp3s, dental age III. — Loc. **LX200009**: HMV 1890, left lunar; HMV 1891, left humerus; HMV 1905, fragmentary cranium with right DP2, DP3, and partial DP4 in alveolus, dental age III. — Loc. **LX200204**: HMV 1887, mandible with both m1s, however, p3s and p4s absent, dental age XIII. — Loc. **LX200037**: HMV 1787, fragmentary right lower tusk. — Loc. **LX200007**: HMV 0013 and 0002, left femurs. — Loc. **LX200008**: HMV 1892 and 1893, right and left dentaries with dp2 and dp3, respectively, dental age II; HMV 1894, right metacarpal IV; HMV 1895, right ulna; HMV 1896, right radius; HMV 1897, right femur; HMV 1911, left humerus; HMV 1899 and 1901, crania with both DP2s, DP3s, and partial DP4s in alveoli, dental age III; HMV 1900, mandible with left dp2, both dp3s, and partial dp4s in alveoli, dental age IV; HMV 1902, cranium with left P3, both P4s, M1s, and partial M2s in alveoli, dental age XIII; HMV 1907, mandible with both p3s, dp4s, and m1s, dental age IX; HMV 1879. 1-3, three fragmentary tusks, two are lower (1 and 2) and one is upper (3); IVPP V18970, almost complete pelvis with partial sacrum.
Precise localities unknown: HMV 1881, atlas; HMV 1884, palate with both DP3s and DP4s, dental age IV; HMV 0539, right ulna; HMV 1906, cranium with both DP2s, DP3s, and DP4s, dental age V; HMV 1456 cranium with associated mandible with DP2s/dp2s, DP3s/dp3s, and partial DP4s/dp4s in alveoli, dental age III; HMV 1903, mandible with both p3s, dp4s, and m1s, dental age X.

TYPE HORIZON. — Early Late Miocene, estimated as 11.1-9.8 Ma (corresponding to the European Vallesian, MN 9/NMU 8).

STRATIGRAPHICAL AND GEOGRAPHICAL DISTRIBUTION. — MN 9-MN 10 (NMU 8-NMU 9), northern China.

DIAGNOSIS. — Neurocranium moderately domed; basicranium moderately erected; mandible with extremely elongated symphysis but not laterally expanded in the distal part; symphysis moderately downwardly deflected and high at the base; upper tusks ventrally bent (at least in the juvenile stage) without lateral enamel band; lower tusks divergent in dorsal view and with tubular internal dentine; exposed length of lower tusks in adults longer than symphyseal length; cross-section of lower tusks dorsally concave and ventrally convex without any concave emargination; DP4/dp4, M1/m1, and M2/m2 bunolophodont and tetralophodont; m3 bunolophodont and hexalophodont; pretrite half-loph(id)s trifoliated; posttrite trefoils weak.

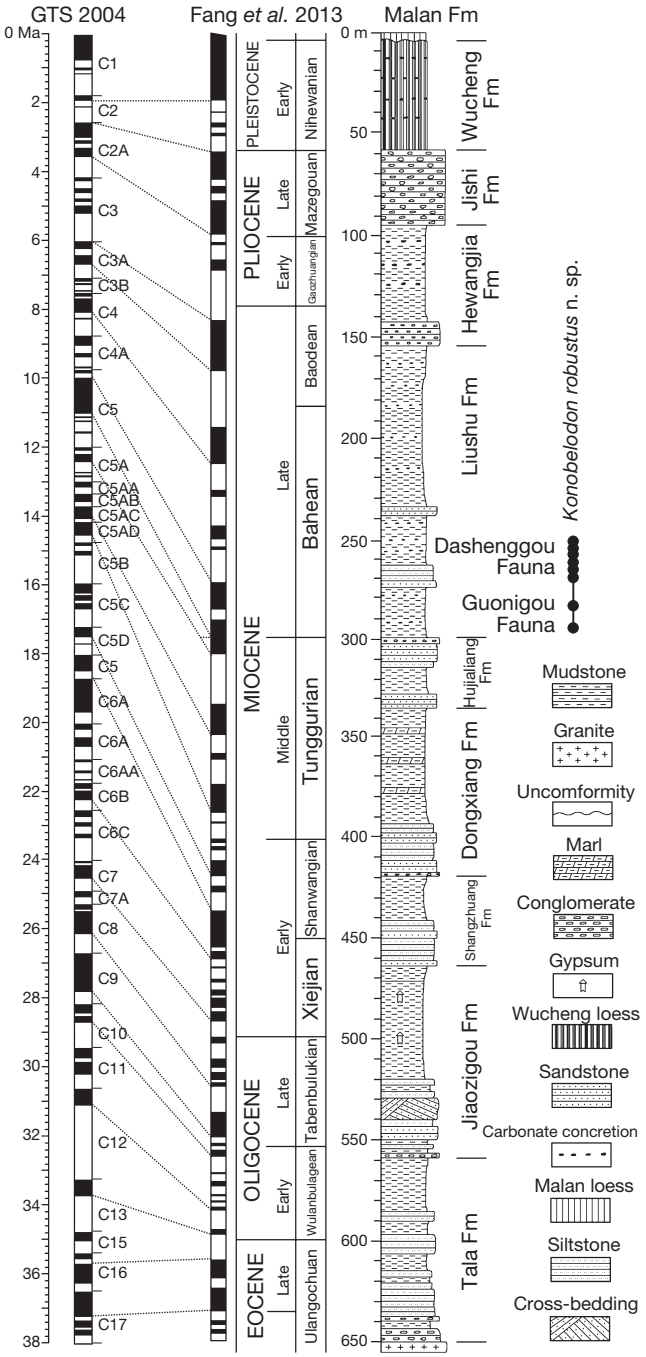

FIG. 2. — Composite stratigraphical section of the Cenozoic deposits of the Linxia Basin with the geological distrubution of *Konobelodon robustus* n. sp. After Deng *et al.* 2013. The magnetostratigraphy is after Fang *et al.* 2003.

DIFFERENTIAL DIAGNOSIS. — Differs from *Konobelodon atticus* in the narrowness of the lower tusks, in the absence of a ventral groove on the lower tusks, in thinner tubular structure in the cross-section of the lower tusk, and in the more divergent lower tusks in juveniles. Differs from *Konobelodon britti* in the smaller size of molars and lower tusks, in the absence of an enamel band in the upper tusks, in the more incipient states of secondary trefoils and pseudo-anancoidy in the cheek teeth. Differs from *Platybelodon* in the relatively domed neurocranium and the relatively erected basicranium, in the not laterally expanded (in the distal part) and downwardly deflected symphysis, in the not posteriorly oblique mandibular rami, in the divergent lower tusks (in

TABLE 1. — Mandibular measurements (in mm) of *Konobelodon robustus* n. sp. The numbers in the brackets are after Tassy (2013).

Specimen	HMV 0004	HMV 1887	HMV 1892	HMV 1893	HMV 0001	HMV 0003	HMV 0011
Maximal length from condyles (1)	–	820	–	–	–	541	–
Length from the anterior to the posterior symphyseal edge (2)	446	314	–	163	401	231	352
Length from the retromolar trigon to the posterior symphyseal edge (3)	–	326	–	–	349	208	296
Length from the angular process to the anterior symphyseal edge (4)	–	700	–	–	872	485	747
Width between two lateral rims of the condyles (5)	–	*c.* 365	–	–	–	318	–
Width at two ramal roots (6)	–	337	–	–	446	292	401
Width of the corpus at the ramal root (7)	–	121	68	61	148	95	120
Width of the corpus at the level of the anterior end of the alveolus (8)	107	700	39	40	96	69	78
Width at the level of the posterior symphyseal edge (9)	245	200	68 × 2	*c.* 92	192	152	187
Width at the anterior symphyseal edge (10)	220	186	–	43.5 × 2	186	114	167
Maximal symphyseal width (11)	220	186	–	46 × 2	186	114	167
Minimal symphyseal width (12)	200	165	41 × 2	40.5 × 2	166	100	158
Maximal width between two interalveolar crests (13)	156	134	–	–	110	–	127
Minimal width between two interalveolar crests (14)	77	57	15.5×2	22 × 2	65	32	54
Width between the medial sides of corpuses at the level of the anterior alveolus (15)	77	64	22 × 2	–	80	42	67
Maximal height of the corpus (16)	137	108	71.5	75	147	93	130
Height of the corpus measured at the ramal root (17)	–	100	63	–	112	79	107
Symphyseal height at its posterior edge (18)	123	105	58	64	122	82	122
Symphyseal height at its anterior edge (19)	64.5	67	–	*c.* 56	80	55	70
Mandibular height from the condyle perpendicular to the ventral border of the corpus (20)	–	*c.* 205	–	–	–	181	–
Maximal ramal depth (21)	–	170	–	–	–	154	–
Depth between angular and coronoid processes (22)	–	187	–	–	–	165	229
Height between angular process and condyle (23)	–	–	–	–	–	146	245
Length from the anterior end of alveolus to the anterior ramal edge (24)	–	196	–	–	200	159	316

Specimen	HMV 1456	HMV 1900	HMV 1903	HMV 1909	HMV 1907	HMV 1908
Maximal length from condyles (1)	–	–	–	–	*c.* 765	–
Length from the anterior to the posterior symphyseal edge (2)	–	170	289	222	275	124.5
Length from the retromolar trigon to the posterior symphyseal edge (3)	196	203	282	242	280	169
Length from the angular process to the anterior symphyseal edge (4)	–	468	–	533	644	–
Width between two lateral rims of the condyles (5)	–	279	–	–	–	–
Width at two ramal roots (6)	239	249	–	272	318	189
Width of the corpus at the ramal root (7)	85	82	111	87	115	60.5
Width of the corpus at the level of the anterior end of the alveolus (8)	60	52	69	54	69	36
Width at the level of the posterior symphyseal edge (9)	127	134	160	138	185	94
Width at the anterior symphyseal edge (10)	–	106	144	110	135	78
Maximal symphyseal width (11)	–	106	144	116	126	78
Minimal symphyseal width (12)	104	105	150	115	135	81
Maximal width between two interalveolar crests (13)	–	57	89	73	102	52
Minimal width between two interalveolar crests (14)	37	31	40	29	45	35
Width between the medial sides of corpuses at the level of the anterior alveolus (15)	45	49	52	52	*c.* 62	43
Maximal height of the corpus (16)	88	81	134	98	75	55
Height of the corpus measured at the ramal root (17)	63	64	90	77	78	47
Symphyseal height at its posterior edge (18)	64	*c.* 75	123	82	83	44
Symphyseal height at its anterior edge (19)	–	36	79	47	41	30
Mandibular height from the condyle perpendicular to the ventral border of the corpus (20)	–	154	–	–	–	–
Maximal ramal depth (21)	–	133	–	163	191	–
Depth between angular and coronoid processes (22)	141	145	–	156	177	–
Height between angular process and condyle (23)	–	132	–	–	–	–
Length from the anterior end of alveolus to the anterior ramal edge (24)	133	127	–	155	200	114

dorsal view), in the longer exposed length and the not much flattened cross-section of lower tusks, and in the tetralophodont DP4/dp4, M1/m1, and M2/m2. Differs from *Amebelodon* in the not laterally expanded (in the distal part) symphysis, in the absence of an enamel band in the upper tusks, in the tetralophodont DP4/dp4, M1/m1, and M2/m2, in the more incipient states of secondary trefoils and of pseudo-anancoidy in the cheek teeth, and in the presence of dentinal tubular structure in the lower tusks. Differs from *Tetralophodon logirostris* in flattened cross-section of lower tusks, and in the presence of dentinal tubular structure in the lower tusks.

ANATOMICAL DESCRIPTION AND COMPARISONS

Mandible (Figs 3; 4; Table 1)

Holotype (Fig. 3). HMV 0004 is an incomplete mandible missing the mandibular rami and the posterior parts of the mandibular corpuses. However, it is the only adult individual in the study material. In dorsal view, the symphysis is almost twice the length of the maximal width; however, the distal part of the symphysis is not transversely expanded. In the basal part, the two interalveolar crests are closed to each other,

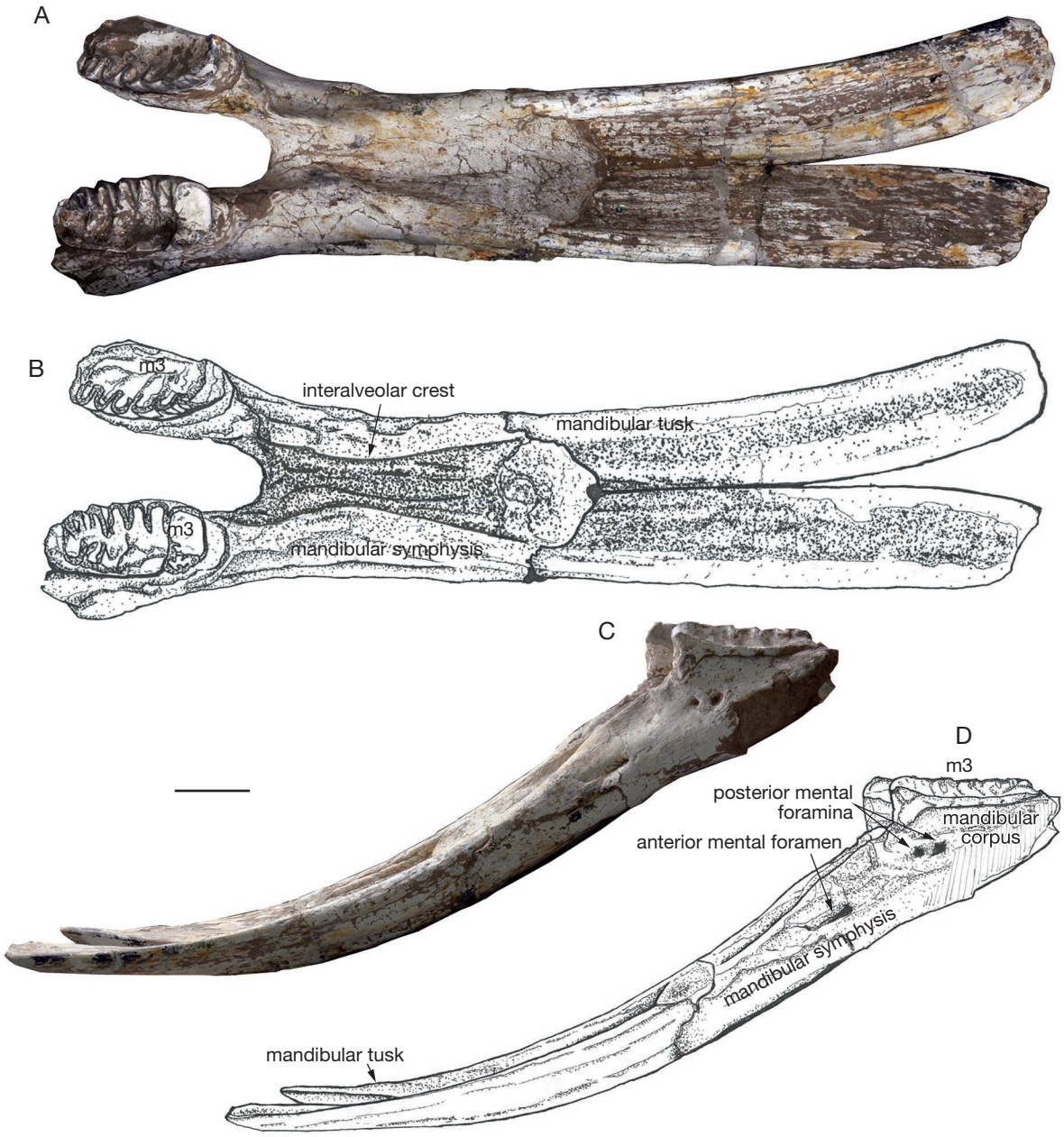

FIG. 3. — Holotype (adult mandible) of *Konobelodon robustus* n. sp.: **A**, HMV 0004, in dorsal view; **B**, sketch and annotations of the panel A; **C**, HMV 0004, in lateral view; **D**, sketch and annotations of the panel C. Scale bar: 100 mm.

forming a narrow medial groove. The interalveolar crests are divergent in the distal part and rapidly reach the anterolateral symphyseal borders. The anterodorsal edge of the symphysis is anteriorly convex rather than straight. In lateral view, the symphysis is moderately downwardly deflected. The height of the symphysis at the base is large, almost equal to the height of the corpus. The posterior mental foramina, which are slightly posterior to the level of the anterior end of the tooth row, are duplicated. The anterior mental foramen is anteroventrally elongated.

Other mandibles (Fig. 4). In addition to the holotype, there are 12 mandibles (HMV 1887, 1892, 1893, 0001, 0003, 0011, 1456, 1900, 1903, 1909, 1907, 1908) in the study material. Except for HMV 1892, 1456, and 1900, all other mandibles possess in situ lower tusks. Within the 12 mandibles, HMV 1887, 0001, 0011, 1903, and 1907 are sub-adults (at least m1 in use), and the others are juveniles. The following description is mainly based on the paratypes HMV 0011 (a sub-adult) and HMV 1909 (a juvenile).

The mandibular ramus is long and shallow with a strong, upward-protruding coronoid process. The angular process is weakly developed, and is at the level of or slightly higher than the occlusal surface of the cheek tooth row. The anterior and posterior ramal borders are perpendicular to the occlusal surface and less posteriorly inclined than those in

TABLE 2. — Cranial measurements (in mm) of *Konobelodon robustus* n. sp. The numbers in the brackets are after Tassy (2013).

Specimen	HMV 1904	HMV 1905	HMV 1456	HMV 1899	HMV 1901	HMV 1902	HMV 1910	HMV 1906
Maximal length from the occipital crest (1)	–	–	424	–	490	559	525	496
Length from the occipital crest to the tip of the nasal (2)	255	196	237	–	220	260	*c.* 240	232
Length of the premaxilla (3)	–	–	180	–	242	279	252	220
Length of the incisive fossa (4)	–	–	138	–	210	237	222	178
Length from the tip of the nasal to the superior rim of the nasal aperture (5)	–	–	34	–	–	27	–	–
Width between two supraorbital processes (6)	335	144×2	242	–	276	293	311	333
Width between two infraorbital foramina (7)	177	–	134	–	131	146	176	172
Width at the distal ends of two premaxillae (8)	–	–	100	–	58.5×2	–	71×2	–
Width of nasal bones at the superior rim of the nasal aperture (9)	98	–	59	–	75	56	88	–
Width of the nasal aperture (10)	195	152	121	–	136	156	165	186
Minimal width between temporal lines (11)	155	160	146	–	113	110	136	135
Maximal length from the condyles (12)	–	–	410	386	–	–	–	495
Length from the anterior margin of the maxillary zygomatic process to the posterior rim of the glenoid fossa (13)	322	–	217	188	263	286	–	239
Length from the posterior margin of the maxillary zygomatic process to the anterior margin of the squamosal zygomatic process (14)	157	113	135	110	157	169	171	160
Length from the anterior grinding tooth to the anterior rim of the choanae (15)	139	119	199	–	179	190	147	245
Length from the anterior rim of choanae to the ventral rim of the foramen magnum (16)	240	–	150	–	–	265	–	223
Length from the anterior to the posterior rims of the maxillary zygomatic process (17)	92	71	75	74	85	95	85	86
Width across two zygomatic arches (18)	203 × 2	–	291	–	–	–	–	–
Width between the lateral rims of the glenoid fossae (19)	160 × 2	–	–	287		325	–	–
Maximal width of the choanae (20)	65.5	–	–	66	45	45	–	66
Maximal width between the medial edge of two tooth rows (21)	69	47	49	61	46	56	55	59
Maximal width between the lateral edge of the tooth rows (22)	173	43×2	130	140	149	152	152	172
Width between the medial edges of the grinding teeth (23)	51.5	–	45	53	43	57	60	53
Minimal width between two interalveolar crests (24)	–	–	36	–	39	52	54	–
Sagittal height of the occipital (25)	225	–	–	–	*c.* 195	224	–	230
Occipital width (26)	176 × 2	–	270			151×2	*c.* 285	*c.* 351
Height of the premaxilla (27)	–	–	44	38	57	58	–	–
Height measured at the anterior grinding tooth (28)	*c.* 132	108	71	66	99	101	–	87
Height of the maxilla ventral to the zygomatic process (29)	59.5	–	24	–	–	65	–	41
Height of the orbit (30)	89.5	–	71	–	64	83	–	70
Height measured from the top of the cranium to the pterygoid process (31)	302	237	213	–	280	350	*c.* 185	299
Length from the condyles to the pterygoid process (32)	*c.* 226	*c.* 163	210	–	*c.* 242	*c.* 320	–	242
Length from the tips of the premaxillae to the pterygoid process (33)	–	–	257	–	312	353	322	272
Length from the anterior margin of the squamosal zygomatic process to the anterior rim of the orbit (34)	199	–	169	–	211	210	213	194
Length from the external auditory meatus to the ventral rim of the orbit (35)	275	–	235	–	–	274	–	–
Height from the pterygoid process to the dorsal rim of the orbit (36)	240	157	173	–	237	269	*c.* 171	202

some taxa such as *Platybelodon grangeri* (Wang *et al.* 2013b) and *Gomphotherium angustidens* (Tassy 2013). The corpus is strong, with a prominent retromolar trigon. The corpus tapers anteriorly in dorsal view and increases in height anteriorly in lateral view. Differing from the duplicated posterior mental foramina in the holotype, there is only one posterior mental foramen in HMV 0011 and HMV 1909. The morphology of the symphyseal part is almost the same as the holotype except that, in lateral view, the downward deflection of the symphysis is not as strong as that in the holotype.

Comparisons. In dorsal view, the mandibular symphysis of *K. robustus* n. sp. does not expand laterally in the distal part. However, in most amebelodontines, the mandibular symphysis expands laterally in the distal part, especially in *Platybelodon* (Fig. 5A-I). This feature is correlated with the morphology of the lower tusks and will be further discussed below. In lateral view, the mandibular symphysis of *K. robustus* n. sp. is downwardly deflected. The deflection is greater than that in *Gomphotherium* and *Platybelodon* (Fig. 5J-L, N), and similar to that in *Amebelodon*, some *Tetralophodon*, and juvenile *K. atticus* (Fig. 5M; also see Schlesinger 1917; Barbour 1927; Mottl 1969; Ferretti *et al.* 2003; Konidaris *et al.* 2014). However, this deflection is significantly smaller than that of *Stegotetrabelodon* and some *Tetralophodon* (Fig. 5P-R).

The ramus of *K. robustus* n. sp. is almost perpendicular to the occlusal plan. This feature is a plesiomorphy as it is observed in *Phiomia*, and also in *Konobelodon britti*, *Amebelodon fricki* Barbour, 1927, and *Gomphotherium* aff. *steinheimense* (Fig. 5L, M). In some longirostrine trilophodont taxa, such as in *G. angustidens* and *Platybelodon grangeri*, the ramus is more posteriorly inclined (Fig. 5J, K). The ramal shape, combined with the cranial shape, is correlated with the distribution of the jaw-closing muscles, and possibly represents different feeding behavior, which will be discussed below.

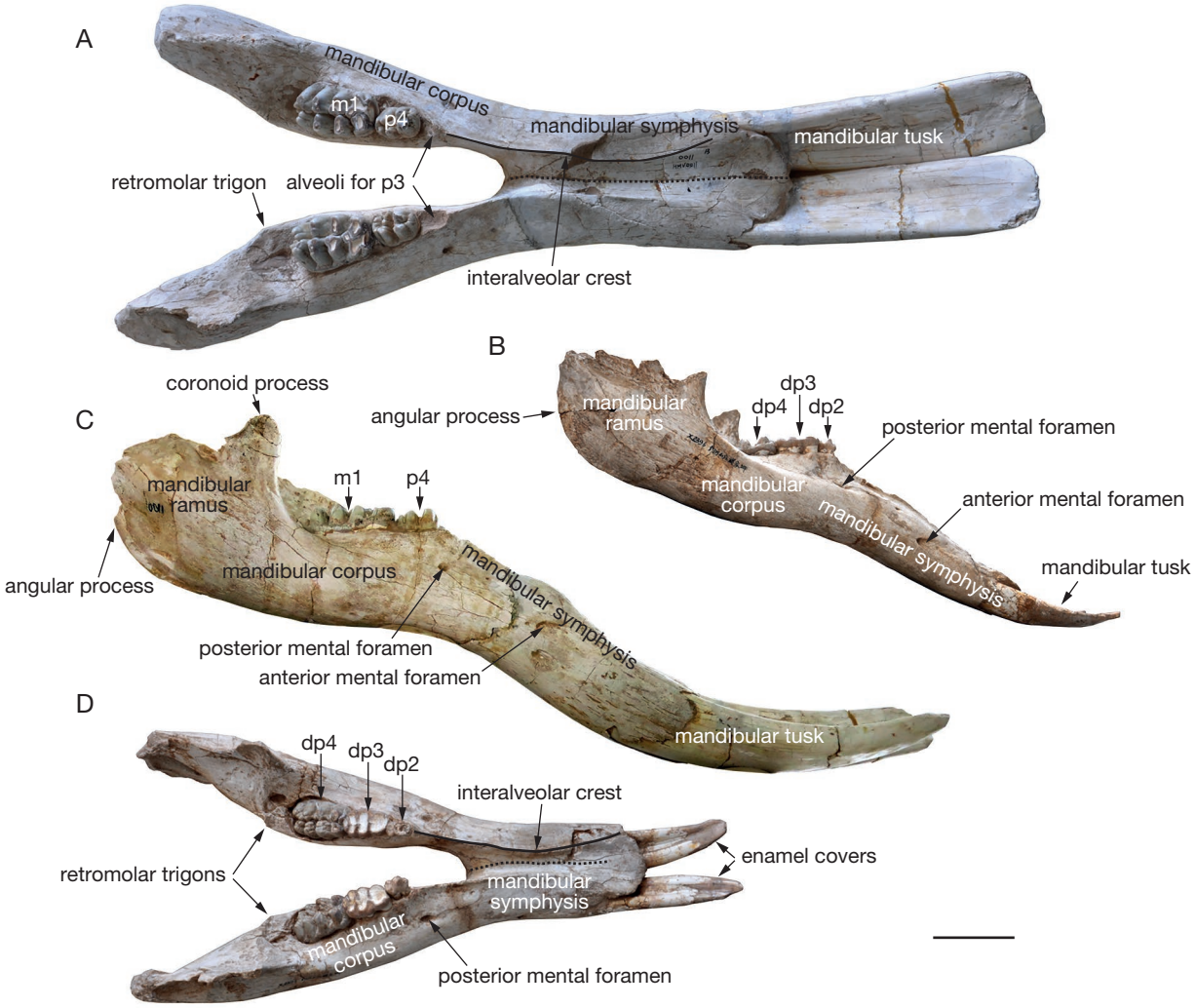

FIG. 4. — Sub-adult and juvenile mandibles of *Konobelodon robustus* n. sp.: **A**, HMV 0011 (paratype), sub-adult in dorsal view; **B**, HMV 1909, (paratype), juvenile in lateral view; **C**, HMV 0011, in lateral view; **D**, HMV 1909, in dorsal view. Scale bar: 100 mm.

Cranium (Fig. 6; Table 2)

There are eight crania (HMV 1904, 1905, 1456, 1899, 1901, 1902, 1910, and 1906) in the study material, of which only HMV 1901 is a sub-adult (possessing P3-M1, and partial M2) and the others are juveniles. The descriptions in dorsal and anterior views, and of the anterior part in ventral view, are based on the paratype HMV 1910; the descriptions in lateral view and of the posterior part in ventral view are based on the paratype HMV 1904.

Dorsal view (Fig. 6A, B). The posterior edge of the neurocranium (the occipital crest) is almost straight. The dorsal plate of the neurocranium is broad and flat, with a large distance between the two temporal lines. In juveniles, the sutures around the frontal bone are very clear. The frontal bone is narrow and extends anterolaterally to the upper rim of the orbits. The anterior edge of the frontal bone is in contact with the nasal and premaxillary bones, and its anterolateral corner is in contact with the maxilla. The nasal bone is triangular with a blunt nasal process. It extends laterally along the superior rim of the nasal aperture and touching the nasal process of the premaxilla. The medial suture between the two nasal bones is also clear. The superior border of the nasal aperture is slightly posterior to the level of the two postorbital processes. The corpus of the premaxilla is long, with a strongly extending nasal process along the inferior and lateral borders of the nasal aperture. On the ventral border of the nasal aperture, the symphysis between the two premaxillae is prominent and encloses a small subnasal fossa (see Ferretti 2010), possibly for the insertion of the mesethmoid cartilage (see Tassy 1994a, b). The incisive fossa between the two premaxillae is narrow and deep. None of the crania have a complete anteriormost part of the alveoli, and thus we do not know whether the premaxilla is laterally expanded anteriorly. The zygomatic arch is not much laterally expanded from the cranium.

Anterior view (Fig. 6C, D). The nasal aperture is low and wide with well-developed perinasal fossae, forming a step-like structure (see Tassy 1994a, b). In the nasal aperture, the opening on the internal lateral surface is very clear. The

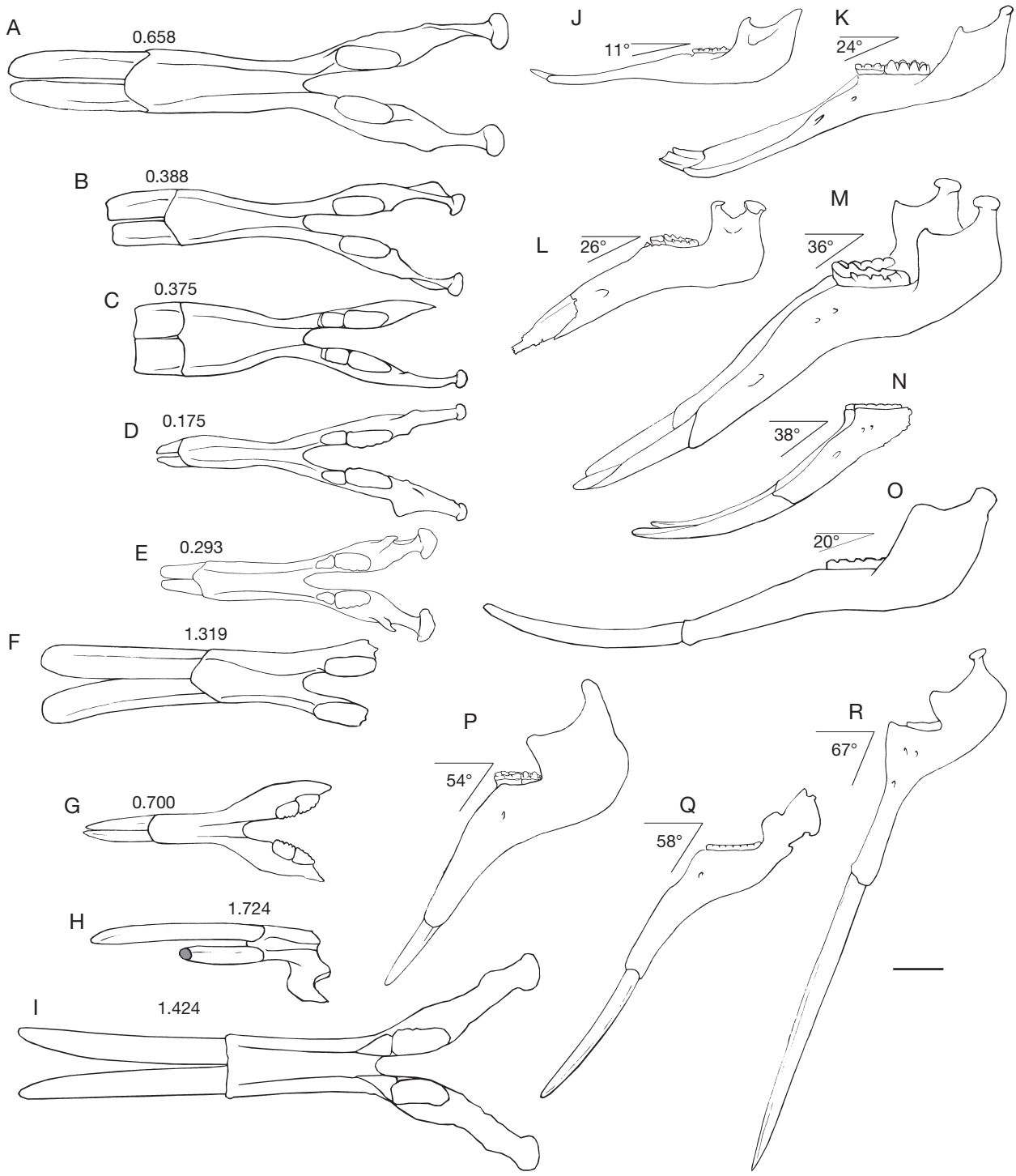

Fig. 5. — Comparison of mandibles of various gomphotheres and stegotetrabelodonts: **A**-**I**, dorsal views, the number in each mandible indicates the ratio of the exposed length of the mandibular tusk to the symphyseal length; **J**-**R**, lateral views, the angle and the number in each mandible indicate the angle between the occlusal surface and the symphyseal axis; **A**, **M**, *Amebelodon fricki* Barbour, 1927, Mr. A. S. Keith of Freedom of Nebraska, US, after Barbour (1927); **B**, *Protanancus tobieni* (Guan, 1988), Anwan, China, after Wang *et al.* (2015); **C**, **K**, *Platybelodon grangeri* (Osborn, 1929), Linxia Basin, China, after Wang *et al.* (2013b); **D**, **J**, *Gomphotherium angustidens* (Cuvier, 1817), En Péjouan, France, after Tassy (2013); **E**, **L**, *Gomphotherium* aff. *steinheimense*, Gweng bei Mühldorf, Germany, after Göhlich (1998); **F**, **N**, *Konobelodon robustus* n. sp., HMV 0004 (holotype); **G**, *Tetralophodon longirostris* Kaup, 1832, Laaerberg, Austria, after Schlesinger (1917); **P**, *Tetralophodon longirostris*, Esselborn, Germany, after Tobien (1978); **H**, **Q**, *Stegotetrabelodon orbus* Maglio, 1970, Lothagam 1, Kenya, after Maglio (1973); **I**, **O**, *Konobelodon atticus* (Wagner, 1857), Pestszentlőrincz, Hungary, after hypothetical reconstruction by Schlesinger (1922); **R**, *Stegotetrabelodon syrticus* Petrocchi, 1941, Sahabi, Libya, after Petrocchi (1943). Scale bar: 200 mm.

perpendicular plate of the ethmoidal bone in the medial position can also be observed. A small lacrymal process is located on the anterior rim of the orbit. In HMV 1910, the right infraorbital foramina are duplicated, as in trilophodont gomphotheres (Tassy 1994b), and the two openings are very close. However, the left infraorbital foramen has only

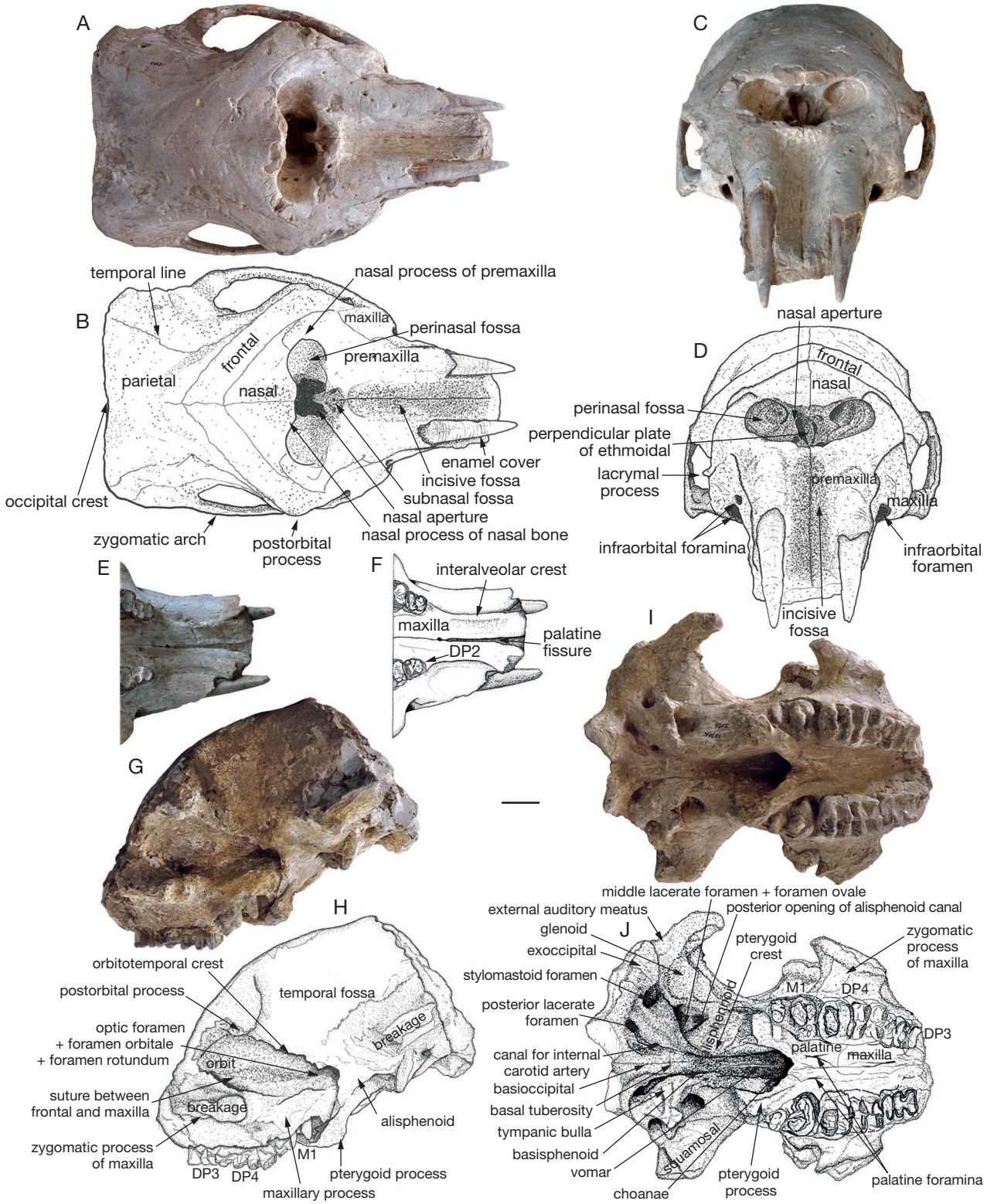

FIG. 6. — Crania of juvenile *Konobelodon robustus* n. sp.: **A**, HMV 1910 (paratype), in dorsal view; **B**, sketch and annotations of the panel A; **C**, HMV 1910, in anterior view; **D**, sketch and annotations of the panel C; **E**, anterior part of HMV 1910, in ventral view; **F**, sketch and annotations of the panel E; **G**, HMV 1904 (paratype), in lateral view; **H**, sketch and annotations of the panel G; **I**, HMV 1904, in ventral view; **J**, sketch and annotations of the panel I. Scale bar: 50 mm.

one opening, as in extant elephants (Tassy 1994b, 2013). The infraorbital foramina aret located just anterior to the zygomatic process of the maxilla.

Ventral view (Fig. 6E, F, I, J). The basioccipital is strong. Anteriorly it is fused with the basisphenoid by a tough basal tuberosity. The basisphenoid tapers anteriorly and is fused with

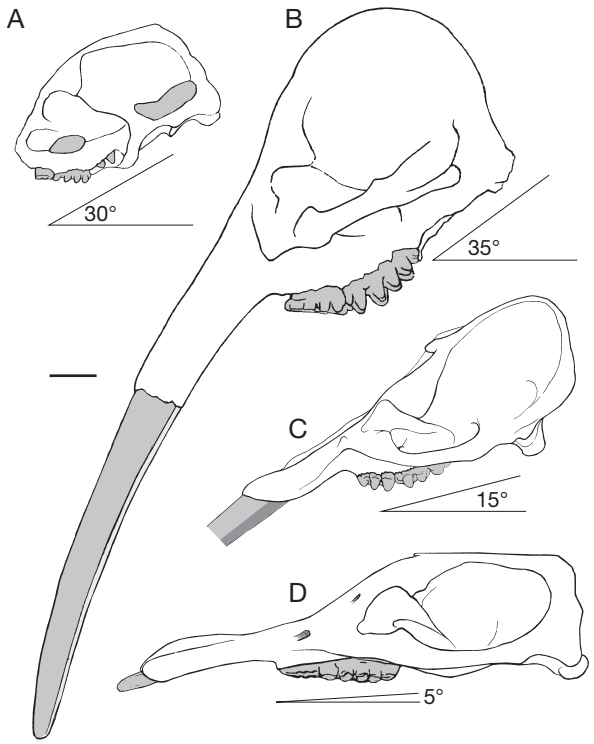

FIG. 7. — Comparison of crania among several gomphotheres. The angle and the number in each cranium indicate the angle between the occlusal surface and the basicranial surface. **A**, *Konobelodon robustus* n. sp., HMV 1904 (juvenile), Linxia Basin, China; **B**, *Paratetralophodon hasnotensis* (Osborn, 1929), Malhuwala, Pakistan, after Tassy (1983b); **C**, *Gomphotherium angustidens* (Cuvier, 1817), MNHN Si37, Simorre, France; **D**, *Platybelodon grangeri* (Osborn, 1929), Linxia Basin, China, after Wang *et al.* (2013bt). Scale bar: 100 mm.

a slim vomer that extends anteriorly into the choanae. The tympanic bulla is large and triangular, lateral to the basioccipital, and surrounded by a series of foramina: a medial and rounded canal for the internal carotid artery; a posterior, large, and irregular posterior lacerate foramen; and a lateral, large and rounded stylomastoid foramen. The middle lacerate and foramen ovale are confluent and located beneath the anterior margin of the bulla, with a large, rounded posterior opening of the alisphenoid canal anterior to the anterior edge of the bulla. The glenoid fossa is relatively flat and the exoccipital is strong and ventrally raised. Between the glenoid fossa and the exoccipital is a shallow groove for the external auditory channel; however, no postglenoid ledge is present. The choanae are oval with a sharp apex on the anterior rim. Lateral to the choanae, a strong pterygoid process is present with a long pterygoid crest posteriorly extending to the anteromedial angle of the tympanic bulla, in which the muscular process is embedded. The palate is narrow with a pair of slit-like palatine foramina. The zygomatic process of the maxilla is dorsally concave on its ventral surface. Two interalveolar crests converge in the middle. The anterior palatine fissure is prominent.

Lateral view (Fig. 6G, H). The neurocranium is moderately domed. The temporal fossa is large and not very anteroposteriorly compressed. The basicranium is moderately erected. In HMV 1904, although broken, the occipital condyle seems

TABLE 3. — Measurements of the upper tusks (in mm) of *Konobelodon robustus* n. sp.

Specimen	Locus	Length (preserved/ exposed)	Maximal diameter	Minimal diameter
HMV 1910	left	29	21	15
HMV 1910	right	28	23	16
HMV 1906	left	303	51	44
HMV 1906	right	279	48	48
HMV 1901	left	93	39	25
HMV 1901	right	50	28	20
HMV 1879.3	?	24	18.5	16

TABLE 4. — Measurements of the lower tusks (in mm) of *Konobelodon robustus* n. sp.

Specimen	Locus	Length (preserved/ exposed)	Width	Medial height	Lateral height	Ratio of medial height/ width
HMV 0004	left	634	104	84	43	0.808
HMV 0004	right	628	125	91	40.5	0.728
HMV 1887	right	275	90	35	27	0.389
HMV 1887	left	–	100	40	28	0.400
HMV 0001	left	–	89	36	–	0.404
HMV 0001	right	–	90	37	–	0.411
HMV 0003	left	–	47	–	19	–
HMV 0003	right	–	51	–	20.5	–
HMV 0011	left	311	92	21.5	21.5	0.234
HMV 0011	right	308	89	31	28.5	0.348
HMV 1787	right	432	117	–	43	–
HMV 1903	left	–	88	–	25	–
HMV 1903	right	–	87	–	18	–
HMV 1909	left	101	46	–	17.5	–
HMV 1909	right	106	46.5	–	20	–
HMV 1907	left	212	62	–	21	–
HMV 1907	right	185	58	–	29	–
HMV 1893	right	120.5	–	15	14	–
HMV 1861	left	165	55	–	9	–
HMV 1908	left	89	29	–	11	–
HMV 1908	right	90	27	–	14	–
HMV 1879.1	left	129	38	–	14	–
HMV 1879.2	?	111.5	26.5	–	17.5	–

posteroventrally protruded. The orbitotemporal crest extends posteroinferiorly to reach the anterior edge of the alisphenoid. A large fissure is located beneath the anterior margin of the alisphenoid, in which the optic foramen, the foramen orbitale, and the foramen rotundum are present. The anterior edge of the alisphenoid turns anteroinferiorly to the pterygoid process, and wraps the posterior end of the posterodorsally erected maxillary process in which an embryo cheek tooth grows. The orbit, in which the transverse suture between the frontal and the maxilla clearly runs from the anterior rim to the anterior margin of the orbitotemporal crest, is rounded. The maxilla inferior to the zygomatic process is low. The occipital surfaces of all known specimens are broken.

Comparisons. The juvenile cranium of *K. robustus* n. sp. has a relatively domed neurocranium and an erected basicranium (Fig. 7A). In the juvenile cranium of *K. atticus* from Pikermi (Greece), the neurocranium is less domed and the basicranium is only moderately erected (Konidaris *et al.* 2014). Kovachev (2004) reported an adult cranium of *K. atticus* from the East

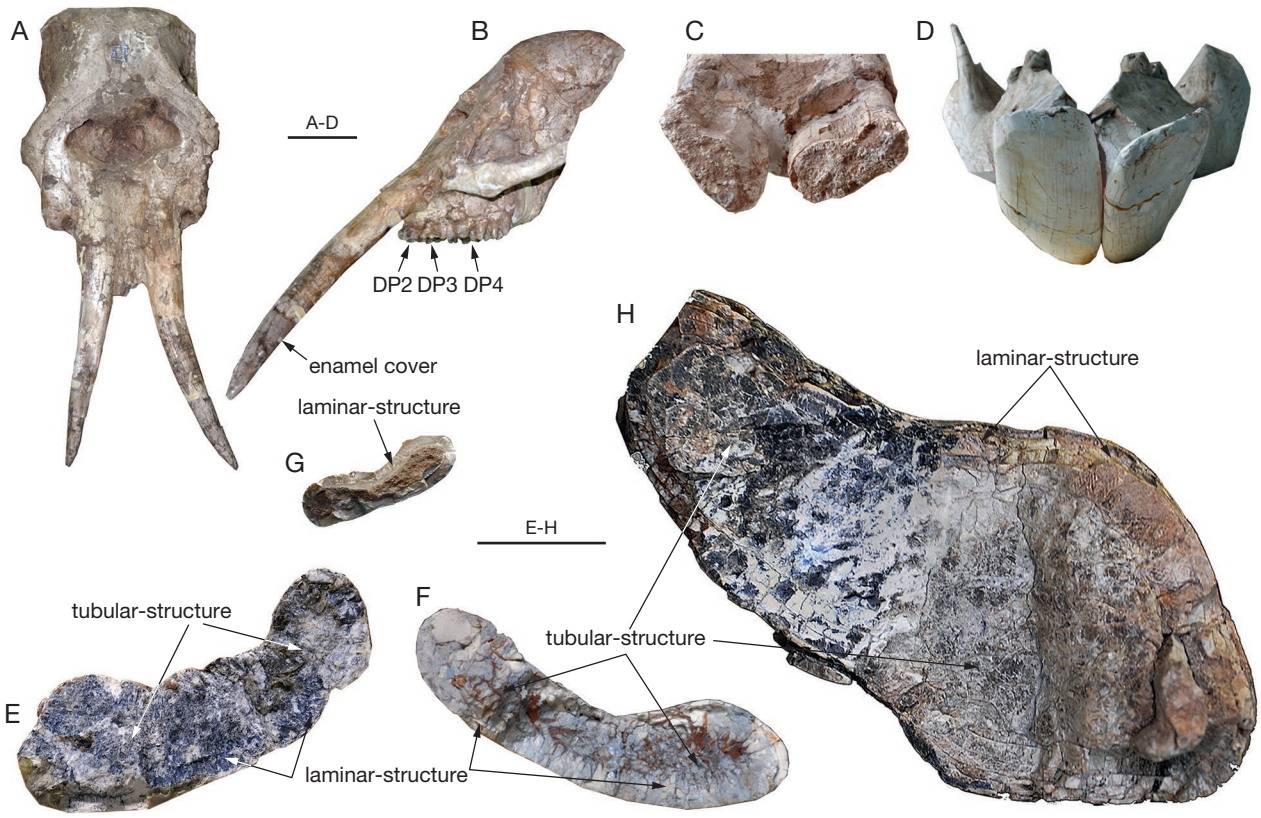

Fig. 8. — Tusks of *Konobelodon robustus* n. sp. and *Konobelodon atticus* (Wagner, 1857): **A-G**, *K. robustus* n. sp.; **A**, HMV 1906, juvenile cranium in antero-dorsal view showing the two divergent upper tusks; **B**, HMV 1906, lateral view showing the ventrally bent upper tusk; **C**, HMV 0001, anterior view showing the two cross-sections of the lower tusks in an oblique angle at the level of the alveoli; **D**, HMV 0011, apical view showing the nearly horizontal apical edge of the lower tusks; **E**, cross-section at the alveolus of a lower tusk (HMV 1887, a sub-adult), in basal view; **F**, cross-section at the middle section (at 165 mm distal to the alveolus) of a lower tusk (HMV 0011, sub-adult), in basal view; **G**, cross-section of a lower tusk (HMV 1879, a juvenile, in basal view); **H**, cross-section of the lower tusk of *K. atticus* (holotype of "*Mastodon grandincisivus*" Schlesinger, 1917, NHMW 1893/0012/0006), from the Late Miocene of Maragheh (Iran). Scale bars: A-D, 100 mm; E-H, 30 mm.

Maritsa Basin (Bulgaria), and its basicranium is also erected like that of *K. robustus* n. sp. However, the cranium figured in Kovachev (2004: fig.1 in pl. 2) shows a concave dorsal outline of the neurocranium in lateral view. We do not know whether this feature is the result of ontogeny, intraspecific variation, or merely an uncorrected reconstruction of the specimen. Nevertheless, a moderately domed neurocranium, an anterioposteriorly compressed temporal fossa, and a moderately erected basicranium have also been found in *Paratetralophodon hasnotensis* (Osborn, 1929) from the Dhok Pathan Formation, Siwaliks, Pakistan (nothing is known about the mandible in this taxon) (Tassy 1983b; see Fig. 7B). Interestingly, in the paratype HMV 1909, duplicated infraorbital foramina were found on its right side (as in trilophodont gomphotheres including amebelodontines) but a single foramen on its left side (as in true elephants) (Tassy 1994b; see Fig. 6C, D). In *Gomphotherium angustidens*, the neurocranium is only slightly domed and the basicranium is also slightly erected (Fig. 7C), but these features are even less developed in known crania of amebelodontines such as *Platybelodon grangeri* (Fig. 7D).

Tusks (Figs 3, 4, 6, 8; Tables 3, 4)

Upper tusk (Figs 6A-F; 8A, B). Three crania (HMV 1910, 1906, and 1901) possess paired upper permanent tusks and HMV 1879.3 is an isolated upper tusk fragment. The upper tusk is strong, oval in cross-section, and clearly ventrally curved. At young ontogenetic stages (younger than dental age IV), the two tusks are almost parallel and have enamel covers (Fig. 6A-F). In older ontogenetic stages (older than dental age V), they are strongly diverging. There is no enamel band on the lateroventral surface of the tusk even when the apical part (which is 145 mm in length from the tip in the left tusk of HMV 1906) is covered by enamel (Fig. 8A, B). The tip of the tusks is simply polished.

Lower tusk (Figs 3; 4; 8C-G). As well as the holotype (HMV 0004), eight mandibles (HMV 1887, 0001, 0003, 0011, 1903, 1909, 1907, and 1908) in the study material possess paired lower permanent tusks, and one (HMV 1893) has a left lower permanent tusk. Another five (HMV 1787, 1893, 1861, 1879.1, and 1879.2) are fragmentary segments.

The cross-section of the permanent tusk is flattened and dorsally concave without a ventral groove (Fig. 8E-G). In juvenile individuals, the tusk is narrow, tapers anteriorly, and has an enamel cover on the tip with many enamel buds on the anterolateral edge. In the adult type specimen HMV 0004, the tusk length is estimated as *c.* 900 mm, including the part in the alveolus. The exposed length is

much greater than the symphyseal length. In lateral view, the tusk is dorsally bent. In dorsal view, the two tusks are divergent. The medial surface is rounded. At the cross-section of the alveoli, the long axes of the two tusks are oblique medioventrally at an angle (Fig. 8C). At the apical ends, the long axes of the two tusks are more horizontal (Fig. 8D), caused by the outward twisting of the tusks. Narrow wear facets are present along both dorsal and ventral sides of the apical end of the tusk, forming a relatively sharp anterior edge.

A tubular structure enclosed by one or several concentric laminae is visible in the cross-section beyond a young ontogenetic age. In the cross-section at the level of the alveoli (Fig. 8E), the tubules are very thin (estimated tubule diameter less than *c.* 1 mm in HMV 1887); and in the cross-section in the middle of the tusk, tubules become thicker (estimated tubule diameter *c.* 1.5 mm in HMV 0011) (Fig. 8F). At a young ontogenetic stage, the tubular structure appears not to be present (Fig. 8G).

Comparisons. No upper tusk of adult *K. robustus* n. sp. is known. In juvenile individuals, an enamel cover is present on the apical part of the upper tusks. It can be assumed that the enamel cover will be used off, as in *K. atticus* from Pestszentlőrincz, Hungary (Schlesinger 1922). However, unlike *K. britti*, no lateral enamel band is present.

The upper tusks of *K. robustus* n. sp. are apparently morphologically distinct from those in the hypothetical cranial reconstruction of *K. atticus* from Pestszentlőrincz (Schlesinger 1922). The upper tusks of *K. robustus* n. sp. are divergent in dorsal view and ventrally bent in lateral view (Fig. 8A, B). However, we do not know the eventual orientation of these tusks in adults *K. robustus* n. sp. It is possible that the reconstruction of the upper tusks by Schlesinger (1922) is not accurate, and the orientation of the upper tusks in *K. atticus* was similar to that found in juvenile *K. robustus* n. sp. from the Linxia Basin.

The lower tusk of *K. robustus* n. sp. is long and flattened, similar to those of *K. atticus* and *K. britti*. The width of the cross-section is much smaller than those of *K. britti* and *K. atticus* (Fig. 9). The medial surface of the lower tusk is rounded, unlike the flattish medial surface in some amebelodontines such as *Platybelodon*. In addition, the dimensions of the lower tusk cross-section of *Torynobelodon loomisi* Barbour, 1929 do not fall into the range of *Platybelodon*, in contrast to that of *T. barnumbrowni* Barbour, 1931, which falls into the range of *Platybelodon*.

The cross-section of the lower tusk of *K. robustus* n. sp. is dorsally concave and ventrally convex, and is without a ventral groove. This feature is similar to *K. britti*. However, in *K. atticus*, the cross-section of the lower tusk is flattened pyriform shape with a ventral and dorsal concavity. A tubular structure enclosed by dentinal layer(s) in cross-section is distributed throughout the entire length of the lower tusk of *K. robustus* n. sp., except in the most juvenile permanent lower tusks. In the proximal cross-section (Fig. 8E), the tubular structure is very fine (estimated tubule diameter less than *c.* 1 mm), and is not easily to be distinguished from the dentinal matrix, whereas in the medial cross-section (Fig. 8F), the tubular structure appears clearer and the dentinal tubules are thicker (estimated tubule diameter *c.* 1.5 mm). The increase in tubule thickness basiapically is similar to that of *K. atticus* and *K. britti*, but, in general, the tubules in *K. robustus* n. sp. are thinner and unclearer than those of the other two species. Tubular structure is a derived feature not present in primitive elephantiforms, and, logically, thicker tubules are more derived than thinner tubules. Furthermore, the stratigraphic range of *K. robustus* n. sp. (MN 9-MN 10) is earlier than *K. atticus* (MN 11-MN 13) and *K. britti* (Hemphillian, *c.* 7 Ma) (Lambert 1990; Konidaris *et al.* 2014). Therefore, *K. robustus* n. sp. is possibly more ancestral than the other species of the genus *Konobelodon*.

The two lower tusks of *K. robustus* n. sp. are divergent in situ. They are more divergent in adults than in sub-adults and juveniles (Figs 3, 4). Thus this feature is strongly correlated with ontogeny. In juvenile *K. atticus* the two lower tusks are slightly convergent (Markov *et al.* 2014: fig. 1). In juvenile *K. robustus* n. sp., the lower tusks are clearly divergent. The medial edge is thicker than the lateral edge. The paratype of *K. britti*, an isolated lower tusk, was identified as a right tusk by Lambert (1990: fig. 3). He also stated that the lateral edge is far thicker than the medial edge (Lambert 1990: 1035). However, comparing the states in *K. robustus* n. sp. and in adult *K. atticus*, we believe that the lower tusk of the paratype of *K. britti* is actually a left tusk.

We have mentioned that, unlike the other amebelodontines, the mandibular symphysis of *K. robustus* n. sp. does not expand laterally in the distal part. This feature is correlated with the morphology of the lower tusks. In *K. robustus* n. sp., at the level of the alveoli, the two long axes of the tusk cross-section are oblique medioventrally, forming an angle (Fig. 8C). Related to that, the mandibular symphysis is high at the base. A narrow, high symphysis helps reducing the twisting stress within the symphysis when an external rotation torque is exerted on the distal part of the lower tusks, as the animal may use its lower tusks for digging as part of the feeding behaviour. To compensate, the two tusks are outwardly twisted, and thus almost horizontal at the apical end (Fig. 8D), as in the other amebelodontines.

The exposed length of the lower tusks in adult individuals of *K. robustus* n. sp. is longer than the symphyseal length (Fig. 5F, N). Because this feature is observed only on one adult specimen, it cannot be ruled out if it is sex-related. This feature is rare in proboscideans, except in stegotetrabelodonts (Fig. 5Q, R, also see Petrocchi 1943; Maglio 1973; Tassy 1999). This character is probably the result of convergent evolution and is also strongly correlated with ontogeny, because in juvenile individuals of *K. robustus* n. sp. the exposed length of the lower tusks is much shorter than the symphyseal length and in sub-adults they are nearly equal in length (Fig. 4).

Cheek teeth (Fig. 10; Tables 5; 6)

DP2 (Fig. 10A). There are 12 DP2s [HMV 1889 (l.), 1905 (r.), 1456 (l. + r.), 1899 (l. + r.), 1901 (l. + r.), 1910 (l. + r.), and 1906 (l. + r.)] in the study material. The DP2 is triangular. The paracone and the protocone are connected with each other; the former is larger and higher than the latter. The metacone and hypocone are small and separated. The cingulum is strong, and surrounds at least the anterior and posterior margins of the tooth.

DP3 (Fig. 10A). There are 18 DP3s [HMV 1884 (l. + r.), 1889 (l.), 1904(l. + r.), 1905 (r.), 0001 (l. + r.), 1456 (l. + r.), 1899 (l. + r.), 1901 (l. + r.), 1910 (l. + r.), and 1906 (l. + r.)] in the study material. The DP3 is rectangular and trilophodont. Although anterior and posterior pretrite central conules are small, pretrite trefoils are visible at least on the first two lophs. In these two lophs, the anterior and posterior pretrite central conules are almost of equal dimensions. The last two lophs are slightly anteriorly curved. The third loph is enlarged with marked ento- and ectoflexus. On the second loph, the metacone (posttrite) is posterior to the hypocone (pretrite); thus, the connection between the successive lophs in the two interlophs is the anterior posttrite half-loph with the next posterior pretrite half-loph. Ptychodonty is present and the posterior cingulum is strong. In some cases, the posterior cingulum is as strong as a fourth loph.

DP4 (Fig. 10B). There are eight DP4s [HMV 1884 (l. + r.), 1889 (l.), 1904(l. + r.), 1905 (r.), and 1901 (l. + r.)] in the study material. The DP4 is rectangular and tetralophodont. Complete pretrite trefoils are developed at least on the first two lophs and slightly anterior curvature is often visible on the last two lophs. The cusps on the lophs and central conules tend to be subdivided into smaller ones and are aligned along the lophs (especially for the posterior lophs), and thus are crest-like. The interlophs are anteroposteriorly compressed. Ptychodonty and the cingulum seem to be reduced relative to the DP3.

P3 (Fig. 10C). There is only one P3 [HMV 1902 (l.)] in the study material. The P3 is small, oval with a strong cusp in the centre, and cingula are surrounding the tooth.

P4 (Fig. 10C). There are only two P4s [HMV 1902 (l. + r.)] in the study material. The P4 is quadrate to oval. The protocone is trifoliate. The paracone is anteriorly oblique to the midline, and higher than the protocone. The metacone and hypocone form a posterior loph. The paracone, metacone and hypocone are subdivided. The anterior and posterior cingula are strong.

M1 (Fig. 10C). There are only two M1s [HMV 1902 (l. + r.)] in the study material. The M1 is rectangular and tetralophodont. The morphology is similar to that of the DP4. Pretrite trefoils are developed on the first three lophs and chevroning is visible on the fourth loph. Cingula are present on the anterior, posterior, and lingual rims of the tooth.

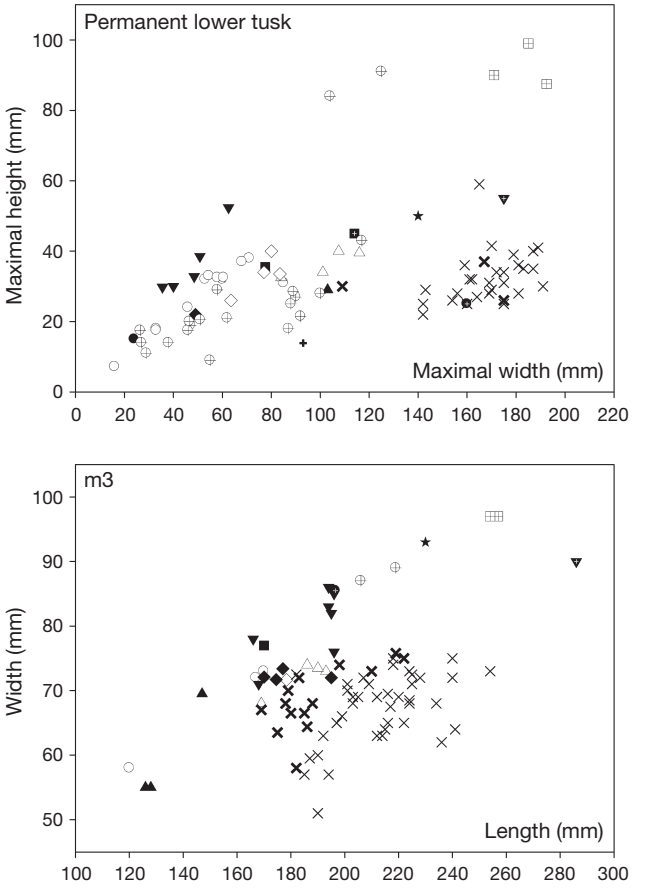

- cf. *Archaeobelodon*
- *Serbelodon barbourensis* Frick, 1933
- *Protanancus brevirostris* Wang, Deng, Tang, Xie, Zhang & Wang, 2015
- *Protanancus macinnesi* Arambourg, 1945
- *Amebelodon fricki* Barbour, 1927
- *Platybelodon danovi* Borissiak, 1928
- *Torynobelodon barnumbrowni* Barbour, 1931
- *Konobelodon britti* (Lambert, 1990)
- *Konobelodon atticus* (Wagner, 1857)
- *Archaeobelodon filholi* (Frick, 1933)
- *Afromastodon coppensi* Pickford, 2003
- *Protanancus tobieni* (Guan, 1988)
- *Protanancus chinjiensis* (Pilgrim, 1913)
- *Platybelodon dangheensis* Wang & Qiu, 2002
- *Platybelodon grangeri* (Osborn, 1929)
- *Torynobelodon loomisi* Barbour, 1929
- *Konobelodon robustus* n. sp.

FIG. 9. — Bivariate plots of various amebelodontine lower tusk and m3 measurements. Data source: *Konobelodon robustus* n. sp., the present contribution; *Konobelodon britti*, from Lambert (1990); *Konobelodon atticus*, from Schlesinger (1917, 1922) and Konidaris *et al.* (2014); cf. *Archaeobelodon*, from Tassy (1986); *Archaeobelodon filholi*, from Tobien (1973); *Serbelodon barbourensis*, from Frick (1933); *Afromastodon coppensi*, from Pickford (2003); *Protanancus brevirostris* and *Protanancus tobieni*, from Wang *et al.* (2015); *Protanancus macinnesi*, from Tassy (1986); *Protanancus chinjiensis*, from Tassy (1983a); *Amebelodon fricki*, from Barbour (1927); *Platybelodon dangheensis*, from Wang & Qiu (2002); *Platybelodon danovi*, from Borrisiak (1929) and Wang *et al.* (2013b); *Torynobelodon barnumbrowni*, from Barbour (1932); *Torynobelodon loomisi*, from Barbour (1929).

TABLE 5. — Measurements of the upper cheek teeth (in mm) of *Konobelodon robustus* n. sp.

Specimen	Locus	Length	Width at the 1st loph	Width at the 2nd loph	Width at the 3rd loph	Width at the 4th loph	Height
HMV 1889	left DP2	25.5	15	19	–	–	14+
HMV 1905	right DP2	32	20	26.5	–	–	16.5+
HMV 1456	left DP2	32.5	23.5	31.5	–	–	22.5
HMV 1456	right DP2	37	23.5	32	–	–	23
HMV 1899	left DP2	34	21	30	–	–	–
HMV 1899	right DP2	39	23.5	30.5	–	–	–
HMV 1901	left DP2	32.5	23.5	30	–	–	–
HMV 1901	right DP2	34	24	30.5	–	–	–
HMV 1910	left DP2	28	–	–	–	–	–
HMV 1910	right DP2	28	–	–	–	–	–
HMV 1906	left DP2	33	20	27	–	–	–
HMV 1906	right DP2	31	21	27	–	–	–
HMV 1884	left DP3	53	–	–	–	–	–
HMV 1884	right DP3	54+	–	–	–	–	–
HMV 1889	left DP3	50.5	28	33	33	–	19+
HMV 1904	left DP3	49	37.5	37.5	41.5	–	–
HMV 1904	right DP3	49.5	35.5	37.5	42	–	–
HMV 1905	right DP3	59	32	37	39.5	–	16+
HMV 0001	left DP3	60	52	52	51	–	36
HMV 0001	right DP3	63	–	49	–	–	36.5
HMV 1456	left DP3	58.5	39	40.5	48	–	23+
HMV 1456	right DP3	62	38.5	41	46	–	25+
HMV 1899	left DP3	59	34	36.5	42	–	–
HMV 1899	right DP3	57	34	36	41.5	–	–
HMV 1901	left DP3	60	37	39	45.5	–	–
HMV 1901	right DP3	63.5	38	38	45	–	–
HMV 1910	left DP3	56	36	37	40	–	–
HMV 1910	right DP3	55	34	37	41	–	–
HMV 1906	left DP3	56	35.5	–	44	–	–
HMV 1906	right DP3	58.5	37	38	44	–	–
HMV 1884	left DP4	83	45	51	49	42.5	32
HMV 1884	right DP4	84	44.5	50.5	48	41	30
HMV 1889	left DP4	90	43	52	52	46	36
HMV 1904	left DP4	87	48	54	54.5	52.5	31
HMV 1904	right DP4	87	49	55	55	52	30
HMV 1905	right DP4	79	–	–	–	–	33.5
HMV 1910	left DP4	85	47	51	45.5	42	30
HMV 1910	right DP4	84	47	51	48	–	29
HMV 1902	left P3	20.5	17	–	–	–	–
HMV 1902	left P4	36	34	35.5	–	–	24.5
HMV 1902	right P4	36	33	35.5	–	–	26
HMV 1902	left M1	94	50	55.5	57	60	28
HMV 1902	right M1	96	52	55	57	59	29

dp2 (Fig. 10D). There are nine dp2s [HMV 1892 (r.), 1893 (r.), 1456 (l. + r.), 1900(l.), 1909 (l. + r.), and 1908 (l. + r.)] in the study material. The dp2 is more slender than the DP2. The protoconid and the metaconid are connected with each other, and the latter is higher. The hypoconid and the entoconid are small and separated. The posterior cingulid is reduced.

dp3 (Fig. 10D). There are 12 dp3s [HMV 1892 (r.), 1893 (r.), 0003 (l. + r.), 1456 (l. + r.), 1900 (l. + r.), 1909 (l. + r.), and 1908 (l. + r.)] in the study material. The dp3 is composed of three lophids, the first one being transversely narrower than the last two. Complete pretrite trefoils are visible at least on the first lophid and the posterior pretrite central conule is larger than the anterior one. On the second lophid, the entoconid (posttrite) is anterior to the hypoconid (pretrite). The second interlophid is anteroposteriorly wider than the first. In the first interlophid, the first posterior pretrite central conule is connected with the second posttrite half-lophid; whereas, in the second interlophid, the second and the third pretrite half-lophids are connected. Ptychodonty and the cingulid are reduced, relative to the DP3. In some cases, the posterior cingulid is as strong as a fourth lophid.

dp4 (Fig. 10E). There are eight dp4s [HMV 0003 (l. + r.), 1903 (l. + r.), 1909 (l. + r.), and 1907 (l. + r.)] in the study material. The dp4 is similar to the DP4, but narrower. The lophids are more oblique anterolingually than those of the DP4. The central conules are more developed than those in the DP4. Complete pretrite trefoils are developed at least on the first three lophids and chevroning is often visible on the last lophid. On the first two lophids, the posterior pretrite central conules are generally larger than the anterior ones. The cusps on the lophids also tend to be subdivided, but the tendency is not as strong as that in the DP4. The posterior cingulid is often composed of two cusps.

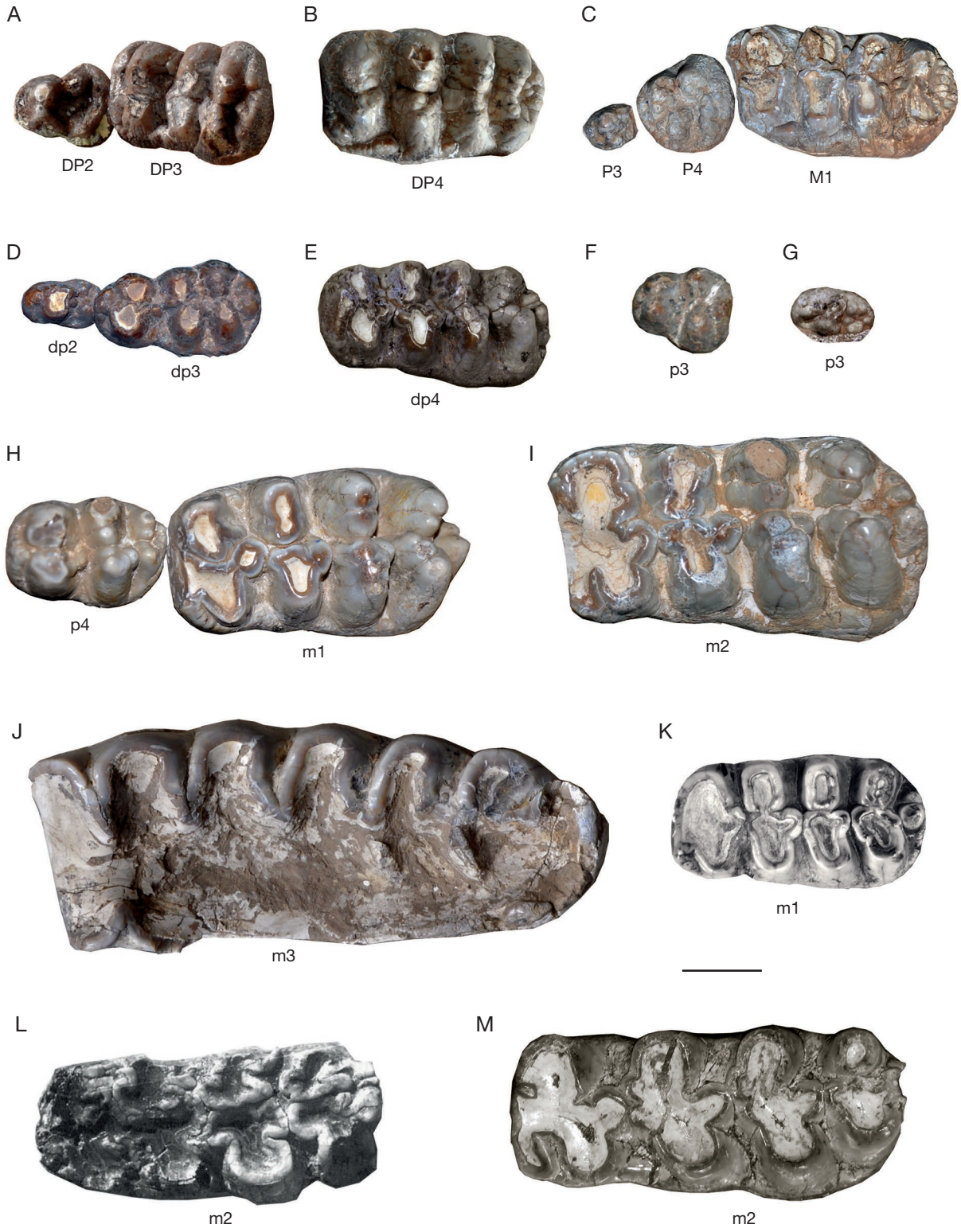

Fig. 10. — Cheek teeth of *Konobelodon robustus* n. sp., *Tetralophodon longirostris* Kaup, 1832, *Platybelodon grangeri* (Osborn, 1929) and *K. britti* (Lambert, 1990), all in occlusal views: **A**-**J**, *K. robustus* n. sp.; **A**, HMV 1456, right tooth row of DP2 and DP3 (horizontally reversed); **B**, HMV 1910, left DP4; **C**, HMV 1902, left tooth row of P3, P4, and M1; **D**, HMV 1908, right tooth row of dp2 and dp3 (horizontally reversed); **E**, HMV 1888, left dp4; **F**, HMV 1907, right p3 (horizontally reversed); **G**, HMV 1888, left p3; **H**, HMV 0011, right tooth row of p4 and m1, (horizontally reversed); **I**, HMV 0001, left m2; **J**, HMV 0004, right m3 (horizontally reversed); **K**, *Tetralophodon longirostris*, left m1, St. Marxer Linie, Austria, from Schlesinger (1917); **L**, *Konobelodon britti*, Blackwater Draw, US, left m2, after Lucas & Morgan (2008); **M**, *Platybelodon grangeri*, left m2, *Platybelodon* Quarry of Tunggur, China, after Wang *et al.* (2013b). Scale bar: 30 mm.

TABLE 6. — Measurements of the lower cheek teeth (in mm) of *Konobelodon robustus* n. sp.

Specimen	Locus	Length	Width at the 1st lophid	Width at the 2nd lophid	Width at the 3rd lophid	Width at the 4th lophid	Height
HMV 1892	right dp2	29	17	19.5	–	–	19+
HMV 1893	right dp2	*c.* 29	–	29	–	–	17+
HMV 1456	left dp2	28	15	18	–	–	24
HMV 1456	right dp2	29.5	15.5	17.5	–	–	24.5
HMV 1900	left dp2	26	14.5	18	–	–	–
HMV 1909	left dp2	26	–	–	–	–	–
HMV 1909	right dp2	27.5	–	–	–	–	–
HMV 1908	left dp2	29	15.5	17.5	–	–	18+
HMV 1908	right dp2	29	17	19	–	–	18+
HMV 1892	right dp3	61	30	34.5	38	–	27.5
HMV 1893	left dp3	62.5	29.5	35	38.5	–	23+
HMV 0003	left dp3	64	29	35	37	–	–
HMV 0003	right dp3	66	29.5	34	38	–	–
HMV 1456	left dp3	58	27.5	34	35	–	–
HMV 1456	right dp3	59	28	34	35	–	–
HMV 1900	left dp3	62	26.5	32.5	35	–	–
HMV 1900	right dp3	63	28	33	36	–	–
HMV 1909	left dp3	55	28	33	33	–	–
HMV 1909	right dp3	58	28	33	33	–	–
HMV 1908	left dp3	64	28	33	34.5	–	23+
HMV 1908	right dp3	63	28	34	36	–	22+
HMV 0003	left dp4	100	43	51	52	–	36
HMV 0003	right dp4	102	43.5	46.5	54	–	35
HMV 1903	left dp4	80	38	41	45.5	46	–
HMV 1903	right dp4	83	–	–	–	48	–
HMV 1909	left dp4	*c.* 80	38	44	46.5	–	–
HMV 1909	right dp4	*c.* 80	–	–	–	–	–
HMV 1907	left dp4	68	–	–	48	43	–
HMV 1907	right dp4	72	–	–	47	43.5	–
HMV 1888	left p3	30	–	–	–	–	–
HMV 1903	left p3	41	23	32	–	–	–
HMV 1903	right p3	42	23	31	–	–	–
HMV 1907	left p3	32.5	22	34.5	–	–	–
HMV 1907	right p3	38	23	31	–	–	–
HMV 0011	left p4	54	34.5	37.5	–	–	32
HMV 0011	right p4	54	34.5	39	–	–	32
HMV 1887	left m1	104	54	56	59	60	38+
HMV 1887	right m1	103	53	60	59	58	*c.* 40
HMV 0011	left m1	114.5	50.5	56.5	61.5	59	*c.* 43
HMV 0011	right m1	113	50	58	63	61	41.5
HMV 1907	left m1	107	51	60	62	–	40
HMV 1907	right m1	107.5	51	60	62.5	–	37+
HMV 0001	left m2	141.5	62.5	66.5	73	80	*c.* 49
HMV 0001	right m2	145.5	59	69	75.5	77	48
HMV 0004	left m3	*c.* 206	–	*c.* 87	–	–	–
HMV 0004	right m3	219	–	*c.* 89	–	–	–

p3 (Fig. 10F, G). There are five p3s [HMV 1888 (l.), 1903 (l. + r.), and 1907 (l. + r.)] in the study material. The p3 from the higher horizon (the Dashenggou fauna) is triangular (Fig. 10F), as in some other tetralophodont gomphotheres, e.g., *Tetralophodon longirostris* and "*T. exoletus*" (Schlesinger 1917; Hopwood 1935). The protoconid and metaconid are connected with each other, whereas the hypoconid and entoconid are separated. The cingulid is on the anterior and posterior edges. However a p3 from the lower horizon (the Guonigou fauna) is oval, although not fully erupted (Fig. 10G).

p4 (Fig. 10H). There are only two p4s [HMV 0011 (l. + r.)] in the study material. The p4 is oval, composed of two complete lophids and a third forming lophid. The protoconid is trifoliate, and the hypoconid lacks the anterior central pretrite conule. The entoconid is subdivided into two cusps. The "third lophid" is also composed of a row of (*c.* 4) conelets, each of which is smaller than that of the second lophid. Anterior and posterior cingulids are also developed.

m1 (Fig. 10H). There are six m1s [HMV 1887 (l. + r.), 0011 (l. + r.), and 1907 (l. + r.)] in the study material. The m1 is rectangular and tetralophodont. Pretrite trefoils are developed at least on the first three lophids and chevroning is present on the fourth lophid. The pretrite half-lophids are mediolaterally elongated or subdivided, especially the posterior two lophids. On the first two lophids, the posterior pretrite central conules are generally larger than the anterior ones. The posttrite half-lophids are generally simple, with a main cuspid and a mesoconelet. The anterior cingulid is weak, and the posterior cingulid is composed of two cuspids. The cementum in the valleys is weak.

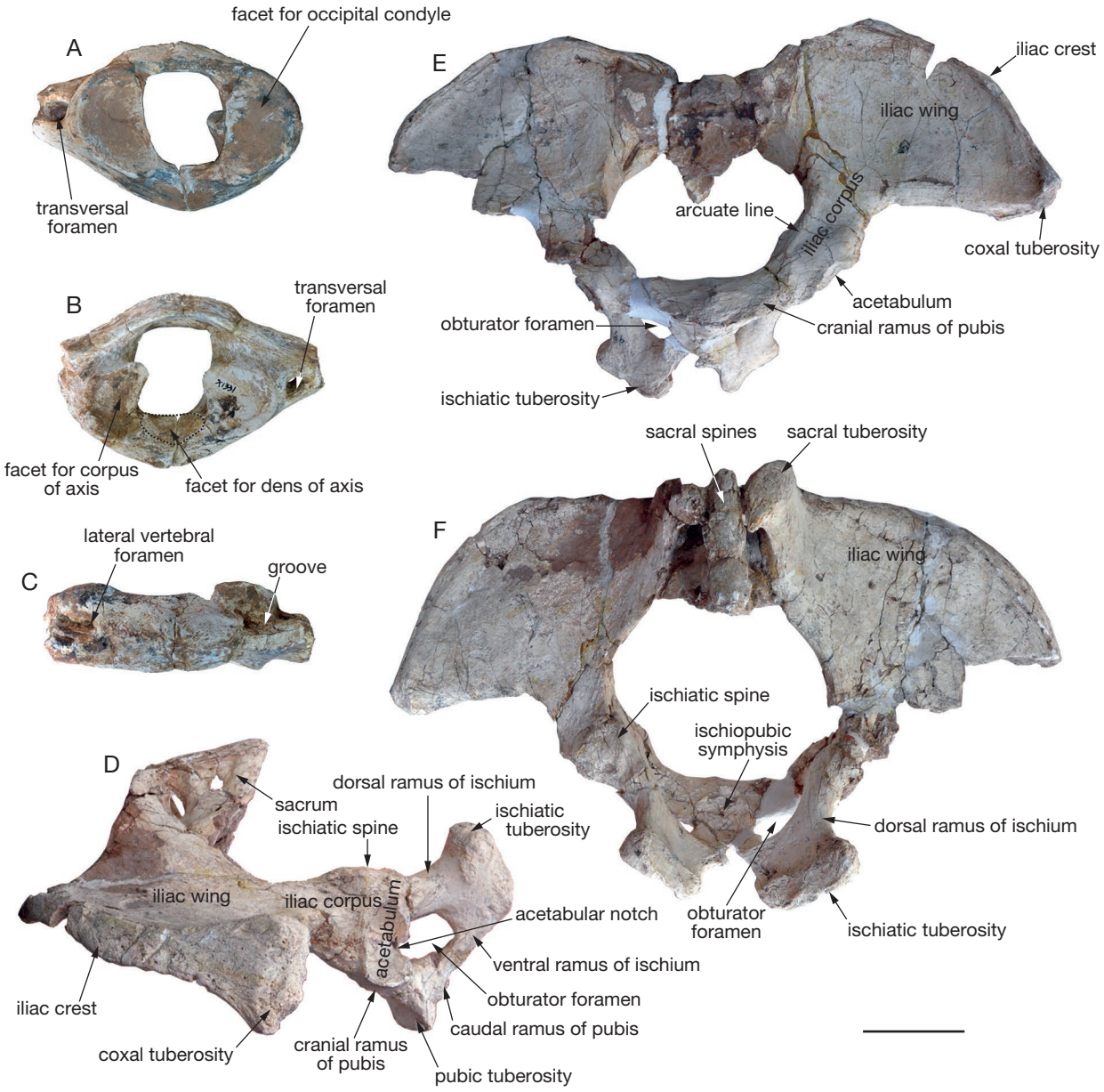

FIG. 11. — Atlas and pelvis of *Konobelodon robustus* n. sp.: **A**-**C**, HMV 1881, atlas, in cranial (**A**), caudal (**B**) and dorsal (**C**) views; **D**-**F**, IVPP V18970, pelvis, in lateral (**D**), ventrocranial (**E**), and dorsal (**F**) views. Scale bar: 100 mm.

m2 (Fig. 10I). There are only two m2s [HMV 0001 (l. + r.)] in the study material. The m2 is generally similar to the m1; however, anterior and posterior posttrite central conules are developed on the first two half-lophids. The tooth also shows a weak tendency to anancoidy and cementodonty.

m3 (Fig. 10J). The only m3s on the holotype HMV 0004 are fully worn. The m3 is composed of six lophids and a not fully developed seventh lophid.

Comparisons. The P3 of *K. robustus* n. sp. is small and oval. It is more regressive than that in *Tetralophodon longirostris* (Schlesinger 1917), in which the P3 is more complex with a quadrate shape. The p3 of *K. robustus* n. sp. of the lower horizon (the Guonigou Fauna) is oval; while that of the upper horizon (the Dashenggou Fauna) is triangular. An oval-shaped p3 has been reported in trilophodont gomphotheres (Tassy 1985; Wang & Qiu 2002; Göhlich 2010; Wang *et al.* 2013c). Therefore, a triangular p3 is a derived feature of tetralophodont gomphotheres. Furthermore, p3 is lost in *Platybelodon grangeri* (Wang *et al.* 2013b).

The cheek teeth of *K. robustus* n. sp. are similar to the typical tetralophodont gomphotheres: three loph(id)s in DP3/dp3, four loph(id)s in the intermediate cheek teeth, and 6-7 lophids in m3. The m3 is close in size with that of *K. atticus* but smaller than that of *K. britti* (Fig. 9). The tooth morphology of *K. robustus* n. sp. and *K. atticus* resembles that of *Tetralophodon logirostris* more than that of *K. britti* and *Platybelodon*

TABLE 7. — Measurements of the atlas (in mm) of *Konobelodon robustus* n. sp.

Specimen	HMV 1881
Maximal length	81
Maximal width (between the two wings)	–
Maximal height	168
Length of the dorsal arch	70.5
Width of the vertebral foramen	77.5
Height of the vertebral foramen	91
Width between two lateral rims of facets for occipital condyles	204
Height of facets for occipital condyles	102
Width between two lateral rims of facets for axis	188
Height of facets for axis	72

TABLE 8. — Humeral measurements (in mm) of *Konobelodon robustus* n. sp.

Specimen	HMV 1882 left	HMV 1891 left	HMV 1911 left
Maximal length	712	655	689
Maximal length from the humeral head	672	–	655
Length from the humeral head to the trochlearis groove	653	631	680
Minimal width of the middle shaft	104	96	111
Minimal perimeter of the middle shaft	375	340	332
Proximal width	213	193	203
Proximal depth	181	196	185
Distal width	210	–	222
Distal depth	123	152	120
Width of the distal trochlea	180	–	187
Thickness index = minimal width of the middle shaft/maximal length	0.146	0.147	0.161

TABLE 9. — Measurements of the ulnae (in mm) of *Konobelodon robustus* n. sp.

Specimen	HMV 0539 right?	HMV 1886 left	HMV 1895 right
Maximal length	–	584	778
Minimal width of the middle shaft	110	91	124
Minimal depth of the middle shaft	133	82	90
Minimal perimeter of the middle shaft	405	273	356
Proximal width	–	–	159
Proximal depth	325	–	284
Width of the olecranon tuberosity	–	–	–
Minimal depth from the anconeal process to ulnal crest	–	–	220
Length of the semilunar notch	106	–	143
Distal width	–	106	159
Distal depth	–	128	185
Width of the distal facet	–	69	124
Thickness index = minimal width of the middle shaft/ maximal length		0.156	0.159

TABLE 10. — Measurements of the radius (in mm) of *Konobelodon robustus* n. sp.

Specimen	HMV 1896 right
Maximal length	700
Length from the proximal facet to the proximalmost point of the distal facet	652
Minimal width of the middle shaft	36
Minimal depth of the middle shaft	84
Minimal perimeter of the middle shaft	240
Proximal width	–
Proximal depth	75
Width of the proximal facet	–
Depth of the proximal facet	64
Distal width	112
Distal depth	164
Width of the distal facet	102
Thickness index = minimal width of the middle shaft/maximal length	0.051

grangeri, although all of them have a tetralophodont m2. Like in *Tetralophodon logirostris* (Fig. 10K) and in *K. atticus*, the interloph(id)s in *K. robustus* n. sp. are anterioposteriorly compressed, and secondary trefoils and pseudo-anancoidy are not marked. In lower molars of *K. britti* (Lambert 1990; Lucas & Morgan 2008), secondary trefoils and pseudo-anancoidy are very pronounced (Fig. 10L). In *Platybelodon grangeri*, only an advanced form of this taxon (in the Tamuqin fauna of the upper Tunggur Formation, see Wang *et al.* 2013b) possesses a tetralophodont m2, whereas the m1 and dp4 are still trilophodont. Even in the tetralophodont m2 of *Platybelodon grangeri*, the fourth lophid is incipient, the interlophids are wider in the anteroposterior dimension, and the contour is narrower than that in *K. robustus* n. sp. (Fig. 10M).

Postcranial bones (Figs 11-15; Tables 7-14)

Atlas (Fig. 11A-C; Table 7). The only atlas (HMV 1881) is elliptical in cranial and caudal views, and compressed craniocaudally. The vertebral foramen is sub-rectangular to oval with a transverse constriction in the medial part. The dorsal arch is thin and low. Most of the transverse processes are broken, and only part of the right one remains, with a rounded opening of the transversal foramen. In cranial view, the articular surface for the occipital condyle is broad, concave, and reniform. In caudal view, the articular surface for the corpus of the axis is sub-quadrate with a marked dorsomedial angle. The facet for the dens of the axis is at the ventromedial part of the ventral arch, and is oblique dorsocaudally. In dorsal view, two interconnected lateral vertebral foramina are located on each side of the dorsal arch with a shallow groove extending from the opening of the lateral vertebral foramen to the cranial opening of the transversal foramen.

Humerus (Fig. 12A-F; Table 8). There are three humeri [HMV 1882 (l.), 1891 (l.), and 1911 (l.)] in the study material. The humerus is very thick. The middle shaft is thin but strongly expanded proximally and distally, and the shaft is strongly twisted clockwise in proximal view for the left humerus. The humeral crest extends distally from the lateral tuberosity and protrudes in the middle, forming a strong deltoid tuberosity, then turns mediocranially to form the medial

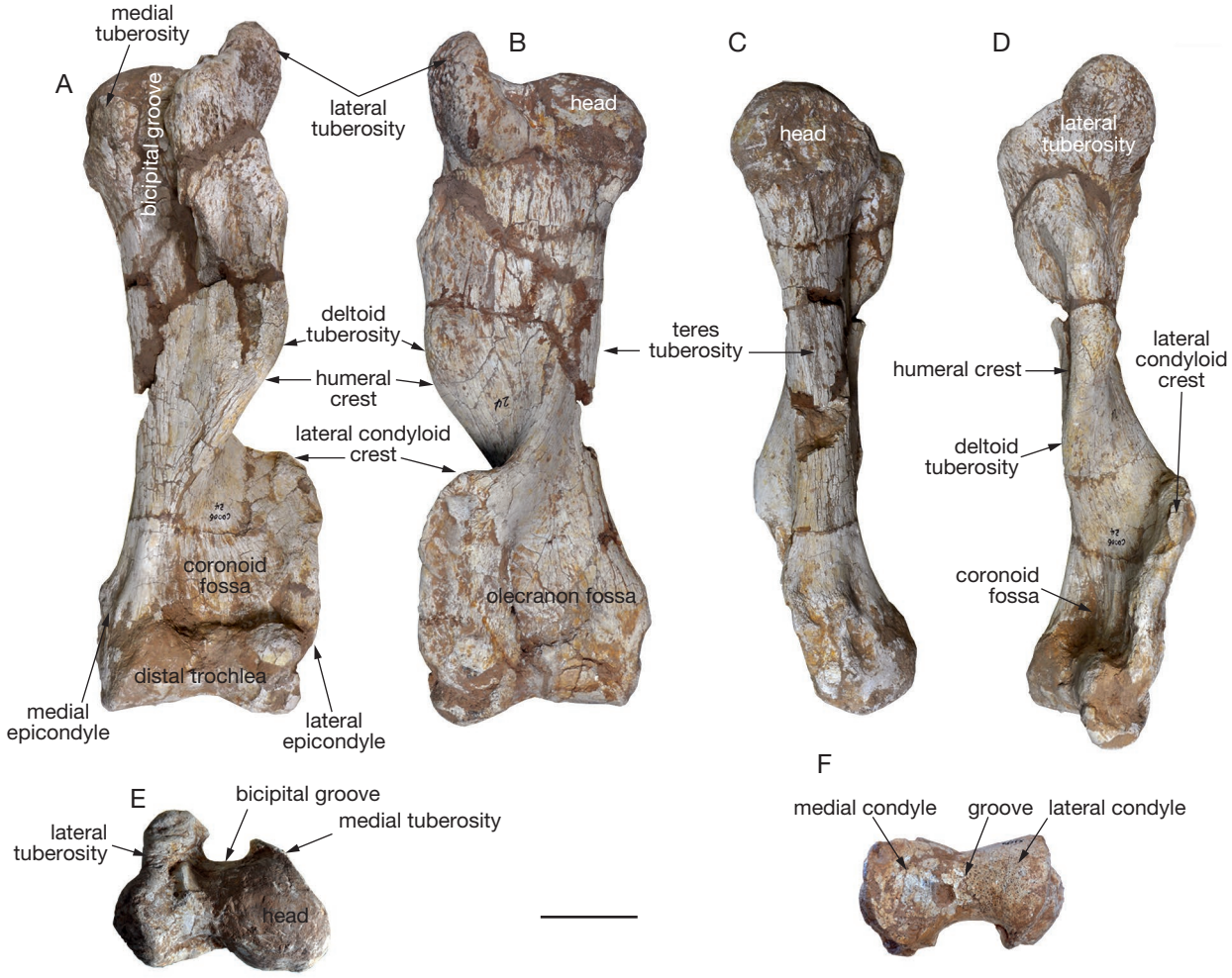

FIG. 12. — Humeri of *Konobelodon robustus* n. sp.: **A**-**E**, HMV 1882, left humerus in cranial (**A**), caudal (**B**), medial (**C**), lateral (**D**) and proximal (**E**) views; **F**, HMV 1911, left humerus in distal view. Scale bar: 100 mm.

border of the coronoid fossa. The lateral condyloid crest initially extends strongly laterally and then makes an acute turn distally, forming an almost right angle and enclosing both a broad coronoid fossa cranially and a broad olecranon fossa caudally. The teres tuberosity is weak. Proximally the humeral head is hemispherical, and the lateral tuberosity is somewhat higher than the head. The medial tuberosity is small. The bicipital groove between the medial and lateral tuberosities is very deep. Distally, the medial condyle of the trochlea is larger than the lateral one, with a wide groove between them. This groove is shallow on the cranial face and deep on the caudal face of the distal trochlea. The lateral depression between the lateral condyle and the epicondyle is more prominent than the medial depression, and the medial epicondyle is more proximally positioned than the lateral one.

Ulna (Fig. 13A-F; Table 9). There are three ulnae [HMV 0539 (?r.), 1886 (l.), and 1895 (l.)] in the study material. The ulna is moderately thick. The cross-section of the shaft is triangular in the proximal part, becoming rectangular in the distal part. In dorsal view, the shaft slightly tapers distally. In lateral and medial views the corpus is volarly concave. In volar view, the ulnar crest is strong and extends throughout the bone. Proximally, the olecranon is swollen, with the medial side more swollen than the lateral side in proximal view. The anconeal process is hook-like and the tip is almost at the same level as the olecranon. The semilunar notch is dorsally concave and smooth. The coronoid process is divided into two lobes by a deep triangular radial notch, and the medial lobe is larger than the lateral one. On both the dorsomedial and dorsolateral sides of the radial notch is a small semilunar facet for the radius. Distally, the facet for the radius is not clear. In distal view, the main facet for the pyramidal is triangular. A small vertical facet meets the dorsomedial side of the pyramidal facet for the lunar. On the lateral side of the distal extremity, the ulnar styloid process is moderately raised.

Radius (Fig. 13G-J; Table 10). The shaft of the only radius [HMV 1896 (r.)] is compressed dorsovolarly and turns distomedially. The mediovolar face of the shaft is concave and rough, facing the corpus of the ulna. The laterocaudal face is convex and smooth. Proximally, the radial tuberosity is moderately developed. The proximal facet for the humerus is triangular and the sharpest angle is laterally

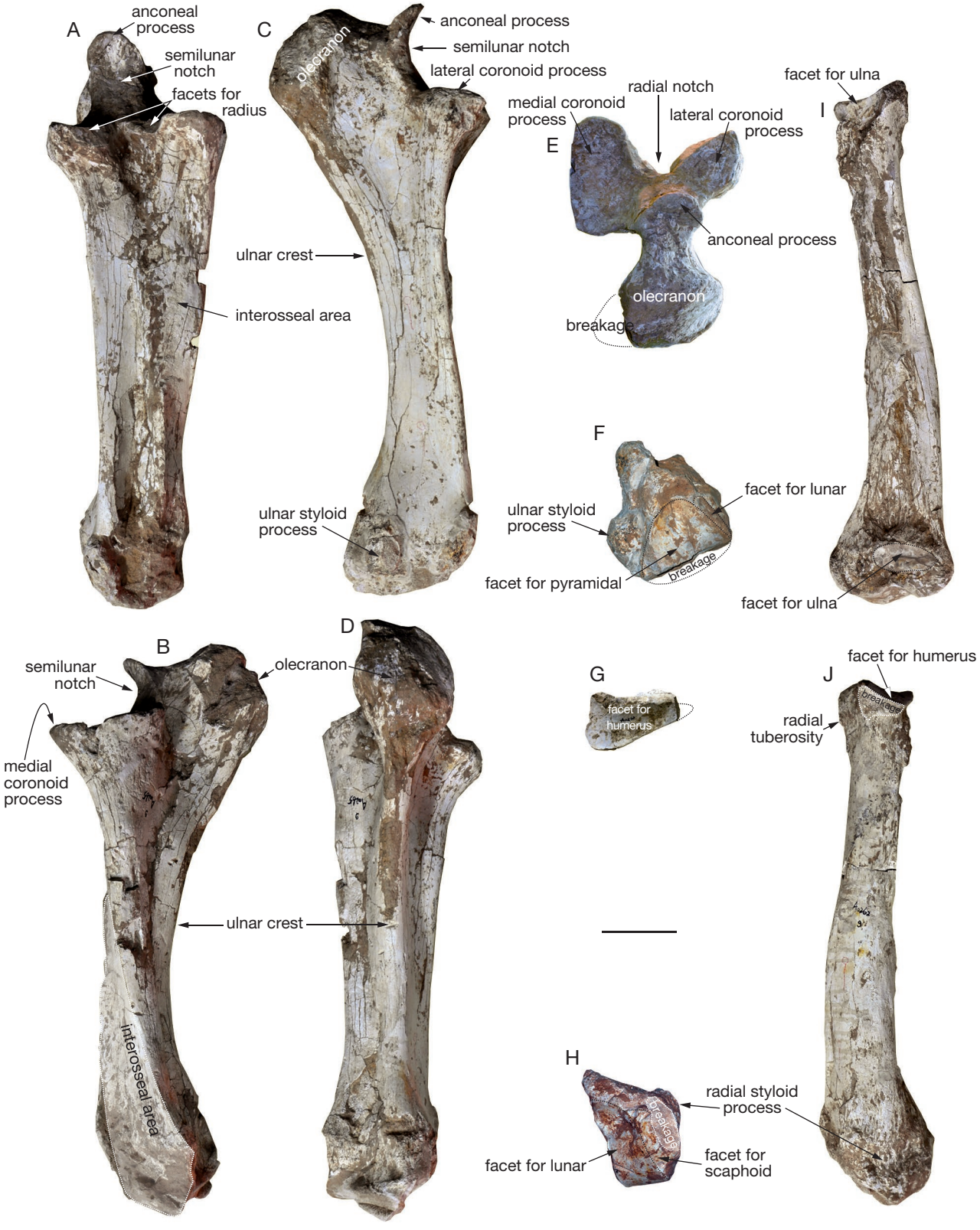

FIG. 13. — Ulna and radius of *Konobelodon robustus* n. sp.: **A**-**F**, HMV 1895, right ulna in dorsal (**A**), medial (**B**), lateral (**C**), volar (**D**), proximal (**E**) and distal (**F**) views; **G**-**J**, HMV 1896, right radius in proximal (**G**), distal (**H**), mediovolar (**I**), laterodorsal (**J**) views. Scale bar: 100 mm.

oriented. The medial edge is almost perpendicular to the dorsal edge, and two lunar facets for the proximal notch of the ulna are present on the proximal extremity of the bone and meet the proximal facet along its medial and latero-volar edges. Distally, the styloid process is weak. The distal articular surface is convex, irregularly tetragonal, and with

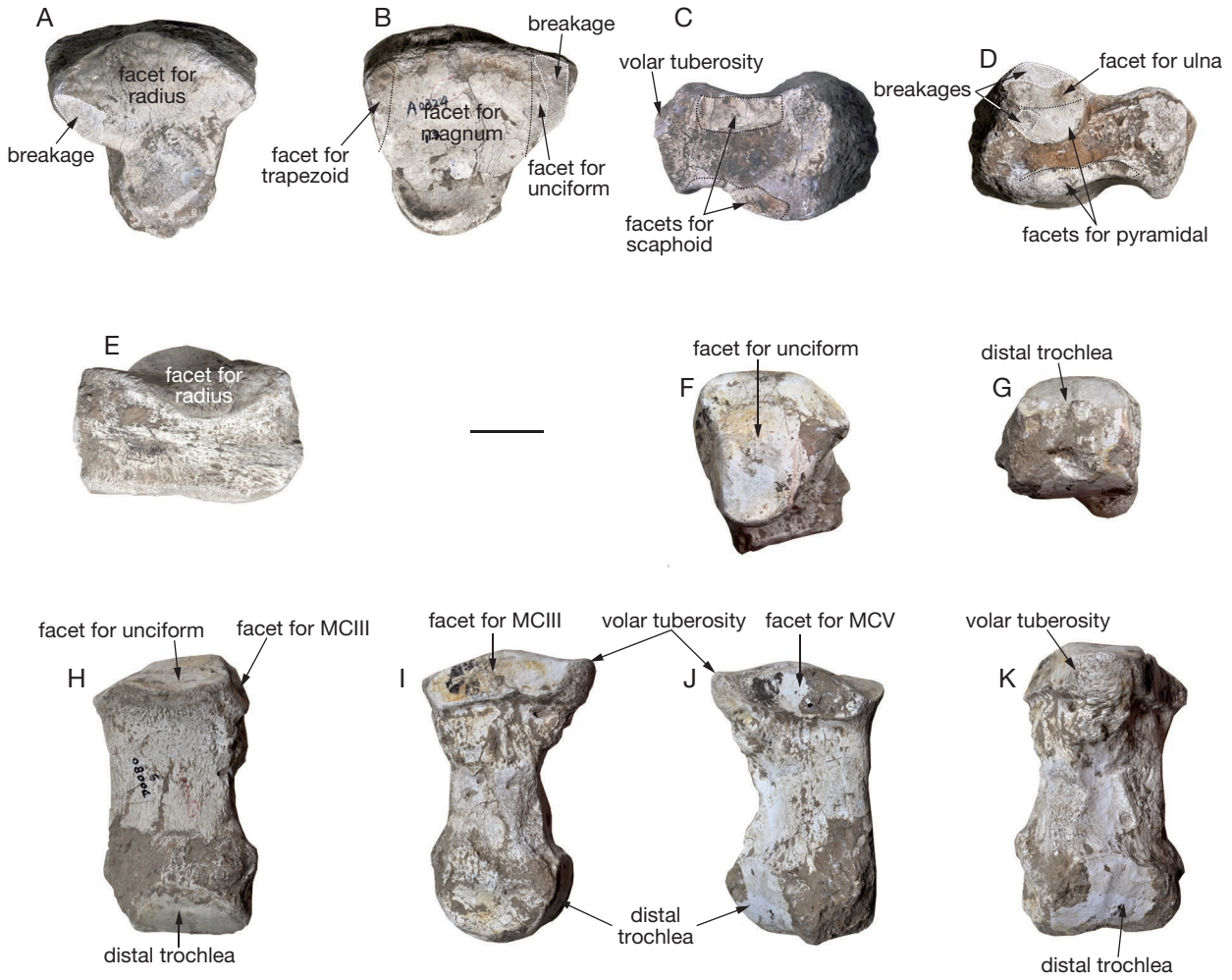

FIG. 14. — Lunar and metacarpal IV of *Konobelodon robustus* n. sp.: **A**-**E**, HMV 1890, left lunar, in proximal (**A**), distal (**B**), medial (**C**), lateral (**D**) and dorsal (**E**) views; **F**-**K**, HMV 1893, left metacarpal IV in proximal (**F**), distal (**G**), dorsal (**H**), medial (**I**), lateral (**J**) and volar (**K**) views. Scale bar: 50 mm.

a sharp dorsolateral angle. The ventral part of the articular surface is divided into two parts by a weak crest, of which the small, medial one is for the scaphoid and the large, lateral one for the lunar.

Lunar (Fig. 14A-E; Table 11). The only lunar [HMV 1890 (l.)] is flat and stout. In proximal and distal views, the shape is triangular. The proximal facet for the radius is saddle-shaped, convex in the dorsal part and concave in the volar part. There is only a small, elliptical facet for the ulna (damaged) along the dorsolateral border of the main facet. The distal facet is concave, most of which is for the magnum, with only a small area of the anterior margin of both the medial and lateral sides joining to the trapezoid and the unciform, respectively. However, there is no clear boundary between these parts of the facet. In dorsal view, the shape is rectangular with a rough anterior face. In medial and lateral views, the dorsal half of the bone is much swollen. The medial facets for the scaphoid are along the proximal and distal margins of the bone and are separated by a notch. Along this notch, the proximal facet is much larger than the distal facet. The lateral facets are also divided into proximal and distal facets by a notch. The proximal facet is sub-circular, dorsally positioned, and is further subdivided by a weak transverse crest, the proximal part of which is for the ulna. The distal part of the proximal facet, and the distal facet along the distal margin of the bone is for the pyramidal. The volar tuberosity is strong.

Metacarpal IV (Fig. 14F-K; Table 12). The only metacarpal IV [HMV 1893 (l.)] is also thick. The shaft is relatively short, with slight anticlockwise torsion in proximal view. It is triangular in cross-section and only slightly expanded in its extremities. The facet for the unciform takes up almost the entire proximal surface. This facet is triangular and convex. The proximal medial facet for metacarpal III and the proximal lateral facet for metacarpal V are dorsovolarly elongated; both meet the proximal facet with a crest. The proximal medial facet is longer than the lateral. The volar tuberosity is large and protruding. The distal extremity is almost equal in width to the proximal one. The width at the epicondyles is wider than that of the trochlea. In distal view, the trochlea is convex dorsally and straight or slightly concave volarly. The volar keel of the trochlea is almost absent.

TABLE 11. — Lunar measurements (in mm) of *Konobelodon robustus* n. sp.

Specimen	HMV 1890 left
Maximal width	150
Maximal depth	149
Maximal height	89
Width of the facet for radius	137
Depth of the facet for radius	130
Width of the distal facet	128
Depth of the distal facet	129
Depth of the proximal facet of the medial side	70.5
Height of the proximal facet of the medial side	28
Depth of the distal facet of the medial side	67
Height of the distal facet of the medial side	31
Depth of the proximal facet of the lateral side	55.5
Height of the proximal facet of the lateral side	56
Depth of the distal facet of the lateral side	80
Height of the distal facet of the lateral side	16

TABLE 12. — Measurements of the metacarpal IV (in mm) of *Konobelodon robustus* n. sp.

Specimen	HMV 1893 left
Maximal length	171
Minimal width of the middle shaft	76
Minimal depth of the middle shaft	54
Minimal perimeter of the middle shaft	220
Proximal width	100
Proximal depth	104
Width of the proximal facet for pyramidal	89
Depth of the proximal facet for pyramidal	102.5
Depth of the proximal facet for metacarpal III	88
Length of the proximal facet for metacarpal III	34.5
Depth of the proximal facet for metacarpal V	78.5
Length of the proximal facet for metacarpal V	28.5
Distal width	103
Distal depth	82
Width of the distal trochlea	82.5
Thickness index = Minimal width of the middle shaft/Maximal length	0.444

Pelvis (Fig. 11D-F; Table 13). The only pelvis (IVPP V18970) is wide with a broad sub-circular aperture. There are partial remains of the sacrum with low and fused spines. The iliac wing is broad and fan-shaped; it is strongly laterally expanded. The sacral tuberosity is thin, upwardly deflected, and turns caudally with a hook-like end. The coxal tuberosity is very thick. The arcuate line is moderately raised in cranioventral view. In lateral view, the pubis, the ischium, and the corpus of the ilium are anteroposteriorly short. The acetabular fossa is oval and its longitudinal axis is almost perpendicular to the main extension of the pelvis. The acetabular fossa is surrounded by a sharp rim with a deep acetabular notch at the middle of the caudal margin. The obturator foramen is sub-circular with the longitudinal axis running almost perpendicular to the acetabular fossa. The cranial branch of the pubis is strong and the caudal branch is thin. The pubic is tightly fused with the other half of the pelvis at the medial side and the pubic tuberosity is thick. The ischium is strongly expanded dorsocaudally in lateral view and strongly extended laterocaudally in caudal view. The cranial branch of the ischium is strong and the caudal branch is thin. The ischiatic tuberosity is very stout and extends craniolaterally-caudomedially.

TABLE 13. — Pelvic measurements (in mm) of *Konobelodon robustus* n. sp.

Specimen	IVPP V18970
Maximal width between the two coxal tuberosities	355 × 2
Maximal length	409
Width of the pelvic aperture	222
Distance between the sacrum and the cranial end of the symphysis	205
Distance between the cranial end of the symphysis and the ventralmost point of the sacral tuberosity	274.5
Distance between the coxal and sacral tuberosities	*c.* 425
Minimal distance between the coxal tuberosity and pelvic aperture	262
Minimal distance between the coxal tuberosity and acetabulum	218
Width between two acetabuli	337
Width between two ischiatic spine	233
Symphyseal length	155
Width between two ischiatic tuberosities	214
Minimal width of the iliac corpus	75
Minimal perimeter of the iliac corpus	*c.* 230
Minimal perimeter of the cranial ramus of pubis	*c.* 140
Minimal height of the dorsal ramus of ischium	44
Minimal perimeter of the dorsal ramus of ischium	*c.* 120
Maximal diameter of the acetabulum	77.5
Maximal diameter of the obturator foramen	74

Femur (Fig. 15A-E; Table 14). There are four femora [HMV 1883 (l.), 0013 (l.), 0002 (l.), and 1897 (r.)] in the study material. The femur is thick. The shaft is long and cylindrical with some craniocaudal compression. The distal two-third of the shaft is slightly convex laterally in cranial or caudal view. The minor trochanter is weak and on the proximal quarter of the medial side of the shaft. On the half of the lateral side of the shaft, a rough and raised tuberosity seems to be for the attachment of the superficial gluteal muscles, the homologue of the third trochanter in perissodactyls. The shaft is enlarged at both extremities. Proximally, the femoral head is markedly hemispheroidal, but relatively small. A rough crest extends laterally from the head and is connected to the major trochanter. The major trochanter is very robust, and more ventrally positioned than the head. It is expanded craniocaudally, and encloses a large, triangular trochanter fossa. Distally, the depressions between the condyles and epicondyles of both sides are deep. The medial and lateral epicondyles are at almost the same level. The distal surfaces are subdivided into a narrow cranial patellar surface and a wide caudal trochlea. The patellar surface is subdivided by a wide, V-shaped valley, and dominated by the medial part. Both parts are oblique craniolaterally-caudomedially. The medial condyle of the distal trochlea is relatively quadrate and larger than the triangular, laterally extended lateral condyle. The two condyles are separated by a deep intercondyloid fossa.

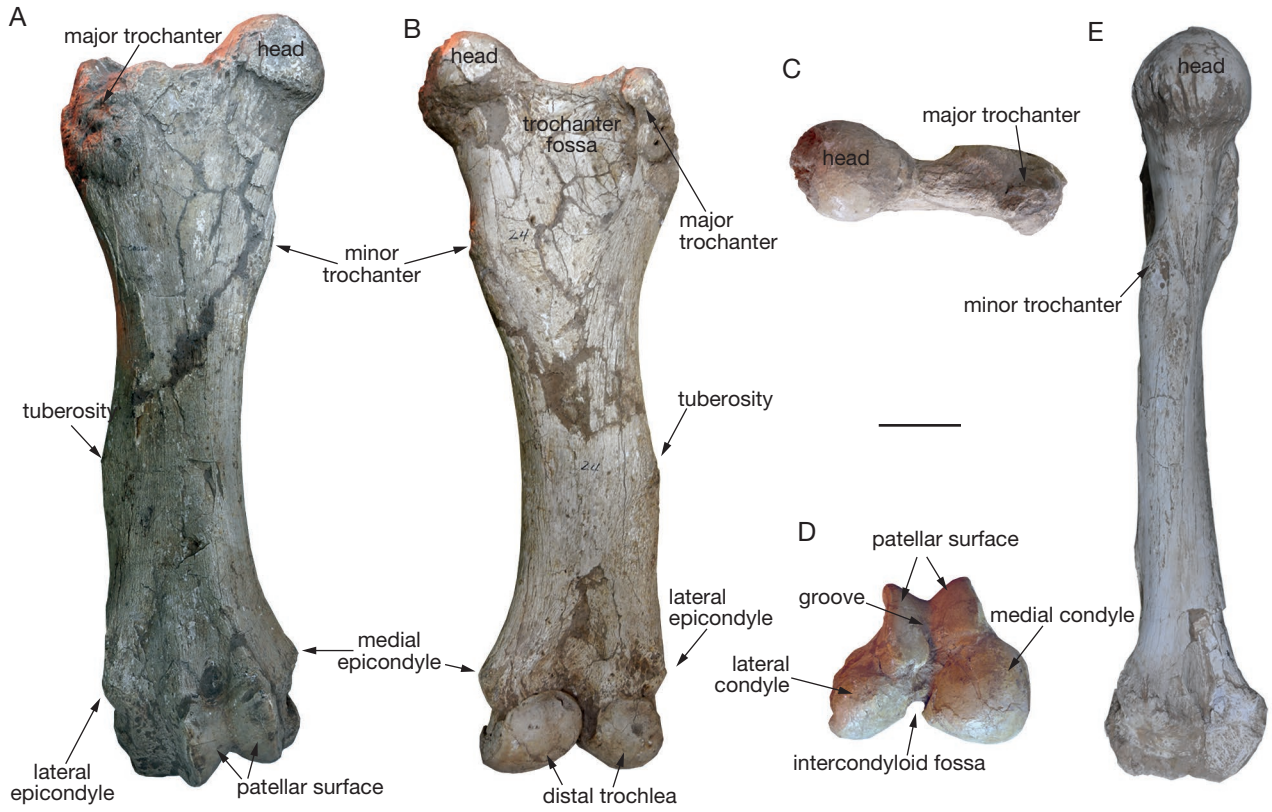

FIG. 15. — Femora of *Konobelodon robustus* n. sp.: **A-D**, HMV 1897, right femur, in cranial (**A**), caudal (**B**), proximal (**C**) and distal (**D**) views; **E**, HMV 1883, left femur in medial view. Scale bar: 100 mm.

TABLE 14. — Femoral measurements (in mm) of *Konobelodon robustus* n. sp.

Specimen	HMV 1883 left	HMV 0013 left	HMV 0002 left	HMV 1897 right
Maximal length from the major trochanter	898	878	–	914
Maximal length from the femoral head	954	938	1025	944
Length from the femoral head to the trochlearis groove	921	907	953	927
Minimal width of the middle shaft	153	166	152	160
Minimal depth of the middle shaft	93	78	99	71
Minimal perimeter of the middle shaft	398	408	415	390
Proximal width	311	347	–	340
Width of the femoral head	158	161	157	140
Depth of the femoral head	137	145	165	122
Distal width	200	235	238	249
Distal depth	221	215	244	216
Width of the patellar surface	72	72	60	104
Width of the distal trochlea	147+	195	*c.* 210	236
Thickness index = minimal width of the middle shaft/maximal length from the femoral head	0.160	0.177	0.148	0.169

Comparisons. We will compare the postcranial bones of *K. robustus* n. sp. with those of other gomphotheres using published data, including *Gomphotherium sylvaticum* Tassy, 1985 (data from Tassy 1977), *G.* aff. *steinheimense* (Klähn, 1922) (data from Göhlich 1998), *Tetralophodon longirostris* (data from Mottl 1969), *Haplomastodon chimborazi* (Proaño, 1922) (data from Ferretti 2010), *K. atticus* from Pestszentlőrincz (data from Schlesinger 1922) and *K. britti* (data from Lambert 1990).

In *K. robustus* n. sp., the sub-rectangular vertebral foramen of the atlas differs from the pear-shaped foramen of *G. sylvaticum*; the thin and low dorsal arch is like that of *T. longirostris*, in contrast to the stout and high arch of *H. chimborazi*; the facet for the dens of the axis is larger and more triangular than that of *G. sylvaticum* and *G.* aff. *steinheimense*. In *K. robustus* n. sp., the iliac crest of the pelvic is not oblique laterocaudally, whereas in *G.* aff. *steinheimense*, *H. chimborazi* and *K. atticus*, the iliac crest is oblique; the oval acetabular fossa differs from the sub-circular acetabular fossa in *K. atticus*. The obturator foramen of *K. robustus* n. sp. is sub-circular with the longitudinal axis running almost perpendicular to the

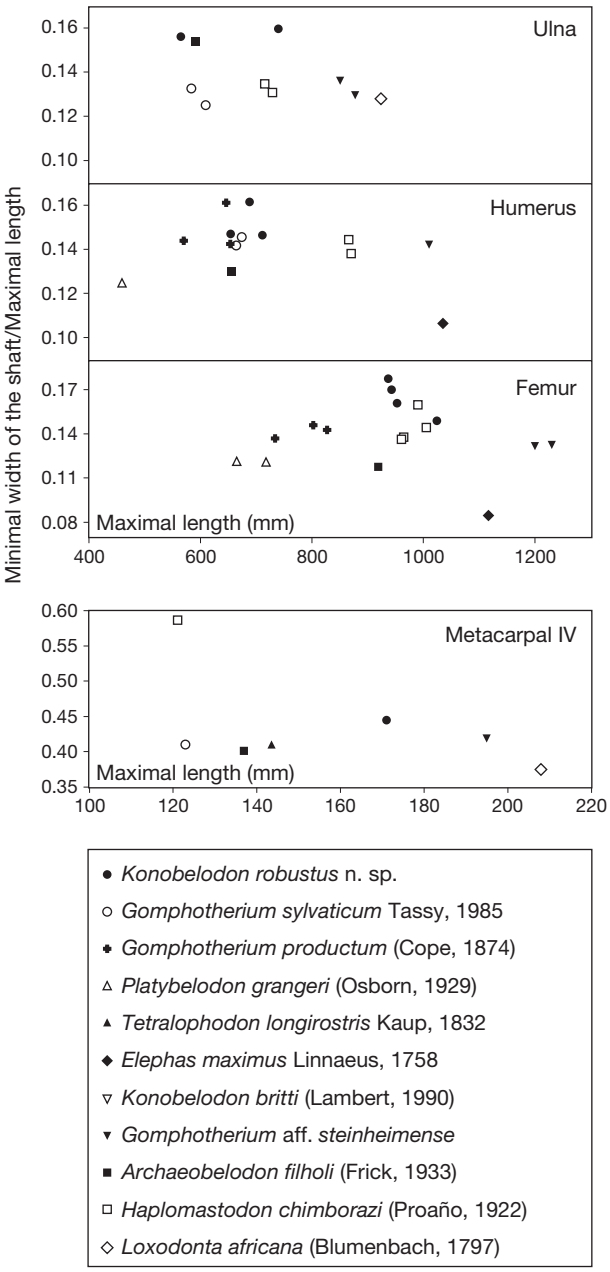

FIG. 16. — Size comparison of limb bones. Data source: *Konobelodon robustus* n. sp., the present contribution; *K. britti*, Lambert (1990); *Gomphotherium sylvaticum*, Tassy (1977); *G.* aff. *steinheimense*, Göhlich (1998); *G. productum*, Christiansen (2004); *Platybelodon grangeri*, in HMV, unpublished data; *Archaeobelodon filholi*, MNHN B-VI-5; *Tetralophodon longirostris*, Mottl (1969); *Haplomastodon chimborazi*, Ferretti (2010); *Elephas maximus* and *Loxodonta africana*, in AMNH.

TABLE 15. — Estimations of body masses (in kg) of *Konobelodon robustus* n. sp. based on length and minimal perimeter of long bones. Equations are linear regression functions with the form $\log_{10}$(mass in kg) = a + b($\log_{10}$X), where X (in mm) are length or minimal perimeter of the middle shaft of long bones. a and b are parameters with following values: **humeral length**, a = –4.145, b = 2.635; **humeral perimeter**, a = –1.598, b = 2.062; **radial length**, a = –3.838, b = 2.634; **radial perimeter**, a = –0.754, b = 2.001; **ulnar length**, a = –4.135, b = 2.674; **ulnar perimeter**, a = –1.349, b = 2.022; **femoral length**, a = –5.568, b = 3.306; **femoral perimeter**, a = –1.606, b = 2.073. Equations and parameters are after Christiansen (2004).

Specimen	Estimation based on the length	Estimation based on the minimal perimeter of the middle shaft	Average
Humerus			
HMV 1882	2351	5125	3738
HMV 1891	1887	4187	3037
HMV 1911	2156	3986	3071
Radius			
HMV 1896	4529	10205	7367
Ulna			
HMV 1886	1830	3775	2802
HMV 1895	3940	6457	5198
Femur			
HMV 1883	3005	6075	4540
HMV 0013	2855	6396	4625
HMV 0002	3737	6625	5181
HMV 1897	2911	5825	4368

acetabular fossa, very unlike the elongated obturator foramen in *K. atticus* and in *G.* aff. *steinheimense*, which is oblique to the acetabular fossa.

In *K. robustus* n. sp., the lateral expansion of the humeral lateral condyloid crest is more prominent than that of *G. sylvaticum*, *G.* aff. *steinheimense*, and *T. longirostris*, but not as prominent as that of *H. chimborazi*; the proximal lateral tuberosity is higher than the humeral head, similar to that of *H. chimborazi*, but distinct from those at almost the same level in *G. sylvaticum*, *G.* aff. *steinheimense*, and *T. longirostris*. In *K. robustus* n. sp., the shape of the radial notch is similar to that of *G. sylvaticum*, and is deeper and narrower than those of *G.* aff. *steinheimense* and *H. chimborazi*. The facets for the radius in the radial notch are separated, on both the dorsomedial and the dorsolateral sides, in contrast with the single, not separated facet in *G.* aff. *steinheimense* and *G. sylvaticum*. Like the radius, the proximal facet for the ulna is separated in *K. robustus* n. sp.; and singular in *G.* aff. *steinheimense* and *G. sylvaticum*. The slight lateral convexity of the distal two-thirds of the femoral shaft in cranial or caudal view in *K. robustus* n. sp. is also visible in *T. longirostris*.

The limb bones of *K. robustus* n. sp. are very robust (Fig. 16). Although relatively short, the humerus, ulna, and femur are thicker than those of known gomphotheres (except the humerus of *Gomphotherium productum* (Cope, 1874), which is almost the same thickness as that of *K. robustus* n. sp.), amebelodontines, and far thicker than those of extant elephants (every vertical coordinate in Fig. 16). The measurements indicate that the femur of *K. robustus* n. sp. is much stouter than that of *K. britti* (Lambert 1990). Only the metacarpal IV is thinner than that of the South American *Haplomastodon chimborazi*, the extremities of which are very specialized (Fig. 16). However, the metacarpal IV is still thicker than in other gomphotheres and extant elephants. The humerus of *K. robustus* n. sp. is relatively short; it is as long as the ulna, and much shorter than the femur (Fig. 16). However, in extant elephants and some brevirostrine gomphotheres (such as *Haplomastodon chimborazi*), the humerus is longer than the ulna, and is close to the length of the femur (Fig. 16). Gomphotheres

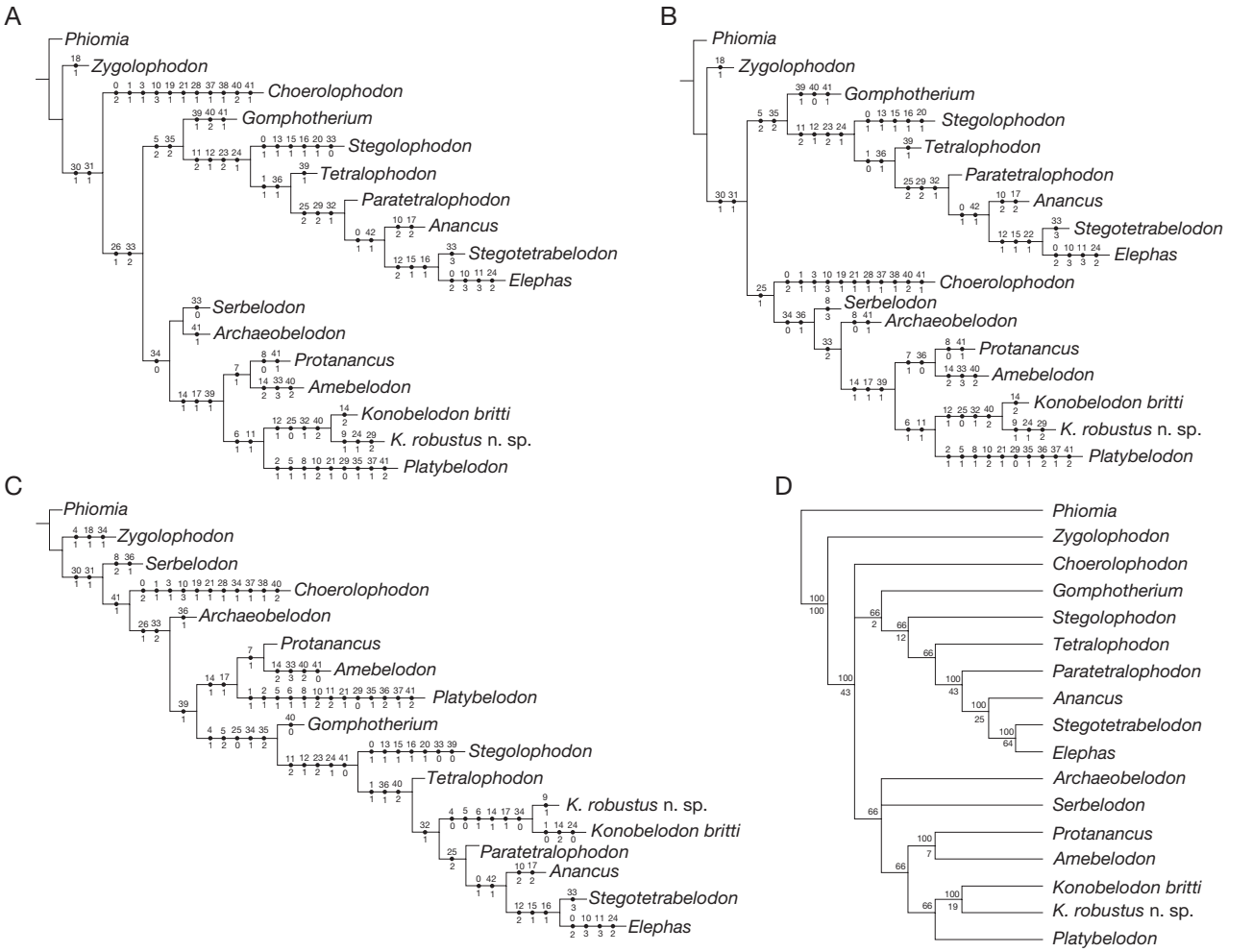

FIG. 17. — The most parsimonious trees resulted from the cladistic analysis of the proboscideans, based on the characters provided in Appendix 1 and the data matrix in Appendix 2. **A**-**C**, MPTs 1-3, the number above each circle represents the supporting character, and that below the character status; **D**, 50% majority rule tree, the regular numbers (%) upper-left to each node represent the supporting rate calculated by the majority rule and numbers lower-left to each node represent the supporting rate calculated by bootstrap analysis.

generally have thicker long bones and a shorter humerus than extant elephants, which has been previously noted, but they do not have as large a body mass as extant elephants (Christiansen 2004). This can be interpreted as resulting from a more columnar standing posture in extant elephants (Christiansen 2007). We estimated the body mass of *K. robustus* n. sp. based on the dimensions of the long bones (Christiansen 2004). The body mass is in the range 2802-7367 kg (Table 15), which is generally larger than that of *Archaeobelodon filholi* (2985-3477 kg), *Gomphotherium angustidens* (2956-3980 kg), and *G. productum* (2304-5429 kg), but smaller than *Cuvieronius hyodon* (2994-7753 kg), *Stegomastodon platensis* (4336-7260 kg) and various true elephantids (Christiansen 2004). Therefore, on the one hand, *K. robustus* n. sp. has a relatively larger body mass than other gomphotheres (except the American brevirostrine gomphotheres), as the limb bones are thicker; on the other hand, its standing posture may not have been as column-like as that of extant elephants and American brevirostrine gomphotheres.

COMPARISON WITH *AMEBELODON*

Since *Konobelodon* was initially established as a subgenus of *Amebelodon* (Lambert, 1990), here comparisons between *K. robustus* n. sp. and *Amebelodon* are further emphasized. Five species have been included in *Amebelodon*, i.e. *A. fricki*, *A. floridanus* (Leidy, 1886), *A. hicksi* (Cook, 1922), *A. paladentatus* (Cook, 1922), and *A. sinclairi* Barbour, 1930 (Lambert, 1990). All of the species are represented by mandibular and/or dental material, and the cranial anatomy of *Amebelodon* is virtually unknown (Lambert 1996). Because *Konobelodon* has been removed from *Amebelodon*, the diagnosis of *Amebelodon* should be confined to the subgenus *Amebelodon* (*Amebelodon*) of Lambert (1990), i.e. trilophodont intermediate cheek teeth; lower tusks with simple laminated internal structure; M3/m3 with five or fewer loph(id)s. All characters are distinct from *K. robustus* n. sp.

A lateral enamel band is present on the upper tusks of *Amebelodon*. This band appears to be absent in *K. robustus* n. sp., although upper tusks of adult individuals of *K. robustus* n. sp. are unknown. In juvenile individuals of *K. robustus* n. sp., the

anterior part of the upper tusks possesses an enamel cap that never extends posterolaterally (Fig. 8A, B).

Lower tusks of *Amebelodon* are narrow, elongated, and flattened with a shallow dorsal concavity, which is similar to those of *K. robustus* n. sp.. However, other features of the lower tusks in *Amebelodon* are notably distinct from those of *K. robustus* n. sp. In *Amebelodon*, besides the absence of internal dentinal tubules, the lower tusks are characterized by a gradually smooth and polished anterior tip without distinct medial and lateral angles; the exposed length of the lower tusks are not longer than the symphyseal length in adult individuals; and the two tusks are convergent (Fig. 5A).

Apart from the number of loph(id)s, the morphology of the cheek teeth in *Amebelodon* and *K. robustus* n. sp. are also different. In the cheek teeth of *Amebelodon*, posttrite trefoils and pseudo-anancoidy are strong, showing a complicated pattern. However, in *K. robustus* n. sp., the posttrite trefoils and pseudo-anancoidy are incipient, the cheek teeth show more "lophodont" features (Fig. 10).

Despite the differences of dental feature within the two group, the mandibular morphology of *Amebelodon* and *K. robustus* n. sp. resembles with each other. In dorsal view, the mandibular symphysis of *Amebelodon* only slightly expand laterally in the distal part, similar to the not laterally expanded symphysis of *K. robustus* n. sp. (Fig. 5A, F). In lateral view, the mandibular symphysis of *Amebelodon* and *K. robustus* n. sp. is downward deflected almost in the same angle (Fig. 5M, N). The mandibular ramus of both *Amebelodon* and *K. robustus* n. sp. is almost perpendicular to the occlusal plan, indicating a similar distribution of the jaw-closing mucles, which possibly represents similar feeding behavior.

Cladistic analysis

The cladistic analyses of Kalb *et al.* (1996) and Ferretti *et al.* (2003) showed that "*M. grandincisivus*" is the sister group of tetralophodont gomphotheres, elephantids, and stegodontids, but is not clustered with the stegotetrabelodontines. However, those analyses did not include the amebelodontines. In our cladistic analysis, we incorporated members of amebelodontines in the dataset. Three MPTs were obtained (tree length = 116, consistency index = 0.586, retention index = 0.625, Fig. 17). As we expected, in all three MPTs *K. robustus* n. sp. clusters with *K. britti*, supporting our generic attribution. In one MPT (Fig. 17C), *Konobelodon* makes up the sister group of *Paratetralophodon*, *Anancus* and other elephantids, and both groups are derived from the *Gomphotherium* stock with other tetralophodont gomphotheres (*Tetralophodon* and *Stegolophodon*). Supporting characters include 11, 12, 23, 24, and 41. This relationship can not be excluded, because the teeth of *K. robustus* n. sp. and *K. atticus* are more similar to those of *Tetralophodon* rather than amebelodontines (however, the shared cheek teeth characters in *K. robustus* n. sp., *K. atticus*, and *Tetralophodon* are plesiomorphies thus not suitable for grouping taxa). Furthermore, in this MPT, other amebelodontines do not cluster either, and constitute a paraphyletic group; after all, the flattened lower tusk is also a plesiomorphy shared with the outgroup *Phiomia*.

In the other two MPTs, all members of the amebelodontines are clustered, forming a monophyletic group (Fig. 17A, B). As an amebelodontine, *Konobelodon* makes up the sister group of *Platybelodon*, supported by characters 6 and 11. These results are more likely to be accepted by most researchers. In *K. robustus* n. sp., the neurocranium is arched and the basicranium is erected, as in derived gomphotheres and elephantids. However, this process seems to have been evolved more than once in different proboscidean clades, and thus possibly represents parallel evolution rather than a true synapomorphy. Tassy (1986, 1999) suggested that "*M. grandincisivus*" is related to *Platybelodon* and Konidaris *et al.* (2014) proposed that *Konobelodon* could have derived from a *Platybelodon* stock. However, we still question the sister-group relationships of *Konobelodon* and *Platybelodon*. *Platybelodon* is a very specialized group within amebelodontines. The horizontal succession of the cheek teeth is notably progressed, and the limb bones of *Platybelodon* are very slender (Fig. 16; also see Wang & Ye 2015), markedly unlike the robust limb bones in *K. robustus* n. sp. The tetralophodont m2 of the two taxa are distinct, as discussed above. The only strong supporting feature is the presence of the tubular structure. Evidence shows that a lower tusk with tubular structure has mechanical advantages for higher load and abrasion (Wang *et al.* 2015), thus this structure may have been independently derived as a result of environmental selection pressure. In our hypothesis, *Konobelodon* is possibly more closely related to *Amebelodon* rather than to *Platybelodon*, as it was originally established as a subgenus of *Amebelodon*, because the similarity of mandibles of *Konobelodon* and *Amebelodon*; however, more evidence is required for this hypothesis. Herein we also provide a 50% majority rule tree (Fig. 17D). This is an acceptable result at the present stage.

Reconstruction of the skull

We reconstructed the juvenile skull of *Konobelodon robustus* n. sp. based on the paratypes HMV 1904 and 1910 (Fig. 18A) and also reconstructed the jaw-closing muscles (see Maglio 1972; Ye *et al.* 1990; Tassy 2014) (Fig. 18B, C). The tip of the upper tusk does not anteriorly surpass the mandibular symphysis and the facial part is not anteriorly elongated. More importantly, the ascending ramus is vertical, unlike the posteriorly oblique ramus in *Platybelodon grangeri* and *Gomphotherium angustidens*. Therefore the composite force of the *m. temporalis* and the deep part of the *m. masseter* is relatively perpendicular to the occlusal surface (Fig. 18B); however, in *Platybelodon grangeri* the same composite force is severely posteriorly oblique. In the latter case, a small moment produced on the mandibular condyle (taken as the pivot of mandibular movements) is resultant and the force component perpendicular to the main extension of the mandible is also relatively small. Therefore, the mandible and lower tusks of *Platybelodon grangeri* are specialized and more suitable for cutting soft vegetation (the main external force is nearly along the main extension of the mandible) than for digging on hard substrate (the main external force is not along the main extension of the mandible but has a considerable perpendicular component). This finding supports the similar conclusion of

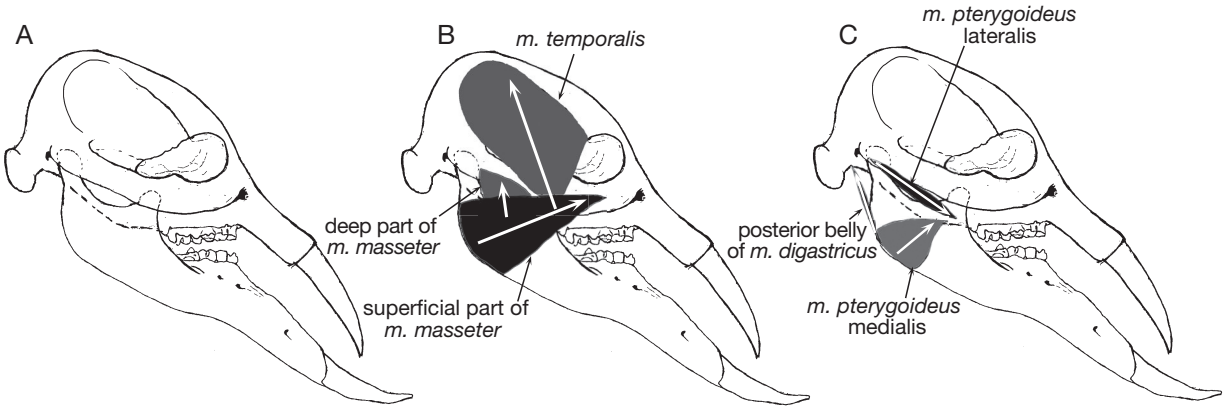

FIG. 18. — Reconstruction of the juvenile *Konobelodon robustus* n. sp.: **A**, reconstruction of the skull; **B**, **C**, reconstruction of the jaw-clossing muscles. The white arrows indicate the contraction direction of the muscles.

Lambert (1992) based on observations of the wear facets and microwear on the lower tusks. The above discussion is only a preliminary qualitative analysis. Further studies should be carried out to better interpret the relationship between feeding behaviors and mandibular morphology of amebelodontines, especially quantitative studies such as finite element methods. Conversely, in elephantids, the lower tusks have been completely lost, and the ascending ramus is anteriorly inclined, yielding a composite force nearly perpendicular to the occlusal surface from the temporal muscle.

CONCLUSIONS

In the present article we studied abundant tetralophodont material from the Late Miocene Liushu Formation of the Linxia Basin, northern China. The flattened lower tusks with tubular internal structure and the tetralophodont intermediate cheek teeth indicate that the specimens should be attributed to the amebelodontine *Konobelodon*. This is the first description of *Konobelodon* in eastern Eurasia. This genus was widespread across the Holarctic realm during the Late Miocene. The unique combination of features (absence of the ventral groove on the lower tusks, very thin tubules in the lower tusks, and incipient secondary trefoils and pseudo-anancoidy in the cheek teeth) differs from the American *K. britti* and the western Eurasian *K. atticus* and permit the establishment of a new species: *Konobelodon robustus* n. sp. Body mass estimates indicate that *Konobelodon robustus* n. sp. was heavier than species of *Gomphotherium* and Amebelodontinae, and lighter than the true elephantids and American brevirostrine gomphotheres. The relatively thicker limb bones but lighter body mass of *Konobelodon robustus* n. sp. than those of elephants indicate a not entirely columnar standing posture. Phylogenetic analysis of genera within Elephantimorpha results in three MPTs. Two trees place *Konobelodon* within the monophyletic Amebelodontinae. The new results enhance our knowledge of the anatomy and phylogeny of *Konobelodon*, and indicate a pronounced diversification and strong parallel evolution in amebelodontines.

Acknowledgements
We thank T. Deng, Z.-X. Qiu, S.-K. Hou, IVPP, China; P. Tassy, Muséum National d'Histoire Naturelle, France; U. Göhlich, Naturhistorisches Museum Wien, Austria; G. Konidaris, University of Tübingen, Germany, G. Koufos, Aristotle University of Thessaloniki, Greece; G. Markov, N. Spassov, National Museum of Natural History, Bulgaria; M. Ferretti, Università di Firenze, Italy; W. Sanders, University of Michigan, USA, and M. Pickford, Collège de France, for discussions and advice on this work, and U. Göhlich and P. Tassy for providing facilities for specimen comparison. We thank G. Konidaris and an anonymous reviewer for many suggestions to improve the article. This work was supported by the National Basic Research Program of China (Grant no. 2012CB821900), the Chinese Academy of Sciences (Grant no. XDB03020104), the National Natural Science Foundation of China (Grant nos 41372001, 41430102, 41202017) and the Key Laboratory of Economic Stratigraphy and Palaeogeography, Chinese Academy of Sciences (Nanjing Institute of Geology and Palaeontology, no Grant no.).

REFERENCES

ANDREWS C. W. 1906. — *A Descriptive Catalogue of the Tertiary Vertebrata of the Fayûm, Egypt*. British Museum (Natural History), London, 324 p.
BAKALOV I. & NIKOLOV I. 1962. — *Les fossiles de Bulgarie. X. Mammifères tertiaires*. Académie des Sciences de Bulgarie, Sofia, 162 p.
BARBOUR E. H. 1927. — Preliminary notice of a new proboscidean *Amebelodon fricki*, gen. et n. sp. *Bulletin of the Nebraska State Museum* 1 (13): 131-134.
BARBOUR E. H. 1929. — *Torynobelodon loomisi*, gen. et n. sp. *Bulletin of the Nebraska State Museum* 1 (16): 147-153.
BARBOUR E. H. 1932. — The mandible of *Platybelodon barnumbrowni*. *Bulletin of the Nebraska State Museum* 1 (30): 251-258.
BORISSIAK A. A. 1929. — On a new direction in the adaptive radiation of mastodonts. *Palaeobiologica* 2: 19-33.
CHOW M.-Z. & ZHANG Y.-P. 1983. — Occurrence of the proboscidean genus *Stegotetrabelodon* in China. *Vertebrata PalAsiatica* 21 (1): 52-58.
CHRISTIANSEN P. 2004. — Body size in proboscideans, with notes on elephant metabolism. *Zoological Journal of the Linnean Society* 140: 523-549. http://dx.doi.org/ 10.1111/j.1096-3642.2004.00113.x

CHRISTIANSEN P. 2007. — Long-bone geometry in columnar-limbed animals: allometry of the proboscidean appendicular skeleton. *Zoological Journal of the Linnean Society* 149: 423-436. http://dx.doi.org/10.1111/j.1096-3642.2007.00249.x

DENG T. 2006a. — Chinese neogene mammal biochronology. *Vertebrata PalAsiatica* 44 (2): 143-163.

DENG T. 2006b. — Neogene Rhinoceroses of the Linxia Basin (Gansu, China). *Courier Forschungsinstitut Senckenberg* 256: 43-56.

DENG T., WANG X.-M., NI X.-J. & LIU L.-P. 2004. — Sequence of the Cenozoic mammalian faunas of the Linxia Basin in Gansu, China. *Acta Geologica Sinica* 78: 8-14. http://dx.doi.org/10.1111/j.1755-6724.2004.tb00669.x

DENG T., QIU Z.-X., WANG B.-Y., WANG X.-M. & HOU S.-K. 2013. — Late Cenozoic biostratigraphy of the Linxia Basin, northwestern China, *in* WANG X.-M., FLYNN L. J. & FORTELIUS M. (eds), *Fossil Mammals of Asia: Neogene Biostratigraphy and Chronology of Asia*. Columbia University Press, New York: 243-273. http://dx.doi.org/ 10.7312/columbia/9780231150125.003.0009

FANG X.-M., GARZIONE C., VAN DER VOO R., LI J.-J. & FAN M. J. 2003. — Flexural subsidence by 29 Ma on the NE edge of Tibet from the magnetostratigraphy of Linxia Basin, China. *Earth and Planetary Science Letters* 210: 545-560. http://dx.doi.org/ 10.1016/S0012-821X(03)00142-0

FERRETTI M. P. 2010. — Anatomy of *Haplomastodon chimborazi* (Mammalia, Proboscidea) from the late Pleistocene of Ecuador and its bearing on the phylogeny and systematics of South American gomphotheres. *Geodiversitas* 32 (4): 663-721. http://dx.doi.org/10.5252/g2010n4a3

FERRETTI M. P., ROOK L. & TORRE D. 2003. — *Stegotetrabelodon* (Proboscidea, Elephantidae) from the Late Miocene of southern Italy. *Journal of Vertebrate Paleontology* 23: 659-666. http://www.jstor.org/stable/4524359

FRICK C. 1933. — New remains of trilophodont-tetrabelodont mastodons. *Bulletin of the American Museum of Natural History* 56: 505-652.

GAZIRY A. W. 1976. — Jungtertiäre Mastodonten aus Anatolien (Türkei). *Geologisches Jahrbuch* 22: 3-143.

GAZIRY A. W. 1987. — Remains of proboscidea from the Early Pliocene of Sahabi, Libya, *in* BOAZ N. T., EL-ARNAUTI A., GAZIRY A. W., DE HEINZELIN J. & BOAZ D. D. (eds), *Neogene Paleontology and Geology of Sahabi.* A. R. Liss., New York: 183-203.

GERAADS D., KAYA T. & MAYDA S. 2005. — Late Miocene large mammals from Yulafli, Thrace region, Turkey, and their biogeographic implications. *Acta Palaeontologica Polonica* 50: 523-544.

GÖHLICH U. B. 1998. — Elephantoidea (Proboscidea, Mammalia) aus dem Mittel- und Obermiozän der Oberen Süßwassermolasse Süddeutschlands: Odontologie und Osteologie. *Müchner Geowissenschaftliche Abhandlungen* 36: 1-245.

GÖHLICH U. B. 2010. — The Proboscidea (Mammalia) from the Miocene of Sandelzhausen (southern Germany). *Paläontologische Zeitschrift* 84: 163-204. http://dx.doi.org/10.1007/s12542-010-0053-1

GOLOBOFF P. A., FARRIS J. S. & NIXON K. C. 2003. — *T.N.T.: Tree Analysis using New Technology.* Program and documentation, available from the authors, and at http://www.lillo.org.ar/phylogeny/ (last access 16th February, 2016).

HOPWOOD A. T. 1935. — Fossil Proboscidea from China. *Palaeontologia Sinica, Series C* 9: 1-108.

KALB J. E., FROEHLICH D. J. & BELL G. L. 1996. — Phylogeny of African and Eurasian Elephantoidea of the late Neogene, *in* SHOSHANI J. & TASSY P. (eds), *The Proboscidea: Evolution and Palaeoecology of Elephants and their Relatives*. Oxford University Press, Oxford: 101-116.

KONIDARIS G. E., ROUSSIAKIS S. J., THEODOROU G. E. & KOUFOS G. D. 2014. — The Eurasian occurrence of the shovel-tusker *Konobelodon* (Mammalia, Proboscidea) as illuminated by its presence in the late Miocene of Pikermi (Greece). *Journal of Vertebrate Paleontology* 34:1437-1453. http://dx.doi.org/10.1080/02724634.2014.873622

KOVACHEV D. 2004. — Cranium of *Stegotetrabelodon* (Proboscideo, Mammalia) from the Neogene in the East Maritsa basin. *Review of the Bulgarian Geological Society* 65: 167-173.

LAMBERT W. D. 1990. — Rediagnosis of the genus *Amebelodon* (Mammalia, Proboscidea, Gomphotheriidae), with a new subgenus and species, *Amebelodon* (*Konobelodon*) *britti*. *Journal of Paleontology* 64: 1032-1040.

LAMBERT W. D. 1992. — The feeding habits of the shovel-tusked gomphotheres: evidence from tusk wear patterns. *Paleobiology* 18 (2): 132-147.

LAMBERT W. D. 1996. — The biogeography of the gomphotheriid proboscideans of North America, *in* SHOSHANI J. & TASSY P. (eds), *The Proboscidea: Evolution and Palaeoecology of Elephants and their Relatives*. Oxford University Press, Oxford: 143-148.

LUCAS S. G. & MORGAN G. S. 2008. — The proboscidean *Amebelodon* from east-central New Mexico and its biochronological significance, *in* LUCAS S. G., MORGAN G. S., SPIELMANN J. A. & PROTHERO D. R. (eds), *New Mexico Museum of Natural History and Science. Neogene mammals*. State of New Mexico, Department of Cultural Affairs, Albuquerque: 89-91.

MADDEN C. T. 1982. — Primitive *Stegotetrabelodon* from latest Miocene of Subsaharan Africa. *Revue de Zoologie Africaine* 96: 782-796

MAGLIO V. J. 1972. — Evolution of mastication in the Elephantidae. *Evolution* 26 (4): 638-658.

MAGLIO V. J. 1973. — Origin and evolution of the Elephantidae. *Transactions of the American Philosophical Society, New series* 63: 1-149.

MARKOV G. N. 2004. — The fossil proboscideans of Bulgaria and the importance of some Bulgarian finds – a brief review. *Historia Naturalis Bulgarica* 16: 139-150.

MARKOV G. N. 2008. — The Turolian proboscideans (Mammalia) of Europe: preliminary observations. *Historia Naturalis Bulgarica* 19: 153-178.

MARKOV G. N., KOVACHEV D. & TASSY P. 2014. — A juvenile mandible of "*Mastodon*" *grandincisivus* Schlesinger, 1917 from Hadzhidimovo, SW Bulgaria. Abstract Book of the VIth International Conference on Mammoths and their Relatives. *Scientific Annals of the School of Geology, Aristotle University of Thessaloniki*, special volume 102: 116.

MOTTL M. 1969. — Bedeutende Proboscidier-Neufunde aus dem Altpliozän (Pannonien) Südost-Österreichs. *Österreichische Akademie der Wissenschaften, Mathemeatisch-naturwissenschaffliche Klasse, Denschriften* 115: 1-50.

OSBORN H. F. 1936. — *Proboscidea: a Monograph of the Discovery, Evolution, Migration and Extinction of the Mastodonts and Elephants of the World. Volume I: Moeritherioidea, Deinotherioidea, Mastodontoidea*. The American Museum Press, New York, 802 p.

PAVLOW M. 1903. — *Mastodon angustidens* Cuv. et *Mastodon* cf. *longirostris* Kaup, de Kertch. *Annuaire Géologique et Minéralogique de la Russie* 4: 129-139.

PETROCCHI C. 1943. — Il giacimento fossilifero di Sahabi. Collezione Scientifica e Documentaria. *A Cura del Ministero Dell'Africa Italiana* 12: 69-167.

PICKFORD M. 2003. — New Proboscidea from the Miocene strata in the lower Orange River Vally, Namibia. *Memoir Geological Survey Namibia* 19: 207-256.

PRADO J. L. & ALBERDI M. T. 2008. — A cladistic analysis among trilophodont gomphotheres (Mammalia, Proboscidea) with special attention to the south American genera. *Palaeontology* 51 (4): 903-915. http://dx.doi.org/10.1111/j.1475-4983.2008.00785.x

QIU Z.-X. & XIE J.-Y. 1998. — Notes on *Parelasmotherium* and *Hipparion* fossils from Wangji, Dongxiang, Gansu. *Vertebrata PalAsiatica* 36 (1): 13-23.

SANDERS W. J., GHEERBRANT E., HARRIS J. M., SAEGUSA H. & DELMER C. 2010. — Proboscidea, *in* WERDELIN L. & SANDERS W. J. (eds), *Cenozoic Mammals of Africa*. University of California Press, Berkeley: 161-251.

SCHLESINGER G. 1917. — Die mastodonten des K. K. Naturhistorischen Hofmuseums. *Denkschriften des K. K. Naturhistorischen Hofmuseums, Geologisch-paläontologische Reihe*. *Wien*, *Ausgegeben* 1: 1-230

SCHLESINGER G. 1922. — Die Mastodonten der Budapester Sammlungen. *Geologica Hungarica, Editio Separata* 2: 1-284.

SHI Q.-Q. 2012. — *Two Late Miocene Ovibovines from Houshan Locality, Linxia Basin, Gansu Province*. Doctoral Dissertation. University of Chinese Academy of Sciences, Beijing, 146 p.

SHI Q.-Q. 2014. — New species of *Tsaidamotherium* (Bovidae, Artiodactyla) from China sheds new light on the skull morphology and systematics of the genus. *Science China: Earth Science* 57 (2): 258-266. http://dx.doi.org/10.1007/s11430-013-4722-2

SHI Q.-Q., HE W. & CHEN S.-Q. 2014. — A new species of *Shaanxispira* (Bovidae, Artiodactyla) from the upper Miocene of China. *Zootaxa* 3794 (4): 501-513. http://dx.doi.org/10.11646/zootaxa.3794.4.1

SHOSHANI J. 1996. — Para- or monophyly of the gomphotheres and their position within Proboscidea., *in* SHOSHANI J. & TASSY P. (eds), *The Proboscidea: Evolution and Palaeoecology of Elephants and their Relatives*. Oxford University Press, Oxford: 149-177.

SISSON S. S. 1953. — *The Anatomy of the Domestic Animals (4th Edition)*. W. B. Saunders Company, Philadelphia, 972 p.

TASSY P. 1977. — Le plus ancien squelette de gomphothère (Proboscidea, Mammalia) dans la Formation Burdigalienne des sables de l'Orléanais France. *Mémoires du Muséum national d'Histoire naturelle, Sér. C, Sciences de la Terre* 37: 1-51.

TASSY P. 1983a. — Les Elephantoidea Miocènes du Plateau du Potwar, Groupe de Siwalik, Pakistan. Ire Partie: Introduction, Cadre chronologique et géographique, Mammutidés, Amébélodontidés. *Annales de Paléontologie* 69: 99-136.

TASSY P. 1983b. — Les Elephantoidea Miocènes du Plateau du Potwar, Groups de Siwalik, Pakistan. IIre Partie: Choerolophodontes et gomphothères. *Annales de Paléontologie* 69: 235-297.

TASSY P. 1985. — *La place des mastodontes Miocènes de l'Ancien Monde dans la phylogénie des Proboscidea (Mammalia): hypothèses et conjectures*. Unpublished Thèse Doctorat ès Sciences, UPMC, Paris, 861 p.

TASSY P. 1986. — *Nouveaux Elephantoidea (Proboscidea, Mammalia) dans le Miocène du Kenya : essai de réévaluation systématique. Cahiers de Paléontologie*. Éditions du Centre national de la Recherche scientifique, Paris, 135 p.

TASSY P. 1994a. — Gaps, parsimony, and early Miocene elephantoids (Mammalia), with a re-evaluation of *Gomphotherium annectens* (Matsumoto, 1925). *Zoological Journal of the Linnean Society* 112: 101-117.

TASSY P. 1994b. — Origin and differentiation of the Elephantiformes (Mammalia, Proboscidea). *Verhandlungen Naturwissenschaftlicher Verains in Hamburg*, *N.F.* 34: 73-94.

TASSY P. 1996. — Who is who among the Proboscidea?, *in* SHOSHANI J. & TASSY P. (eds), *The Proboscidea: Evolution and Palaeoecology of Elephants and their Relatives*. Oxford University Press, Oxford: 39-48.

TASSY P. 1999. — Miocene elephantids (Mammalia) from the Emirate of Abu Dhabi, United Arab Emirates: Palaeobiogeographic Implications, *in* WHYBROW P. J. & HILL A. (eds), *Fossil Vertebrates of Arabia*. Yale University Press, New Haven: 209-233

TASSY P. 2013. — L'anatomie cranio-mandibulaire de *Gomphotherium angustidens* (Cuvier, 1817) (Proboscidea, Mammalia): données issues du gisement d'En Péjouan (Miocène moyen du Gers, France). *Geodiversitas* 35 (2): 377-445. http://dx.doi.org/10.5252/g2013n2a6

TASSY P. 2014. — L'odontologie de *Gomphotherium angustidens* (Cuvier, 1817) (Proboscidea, Mammalia): données issues du gisement d'En Péjouan (Miocène moyen du Gers, France). *Geodiversitas* 36 (1): 35-115. http://dx.doi.org/10.5252/g2014n1a2

TASSY P. & DARLU P. 1986. — Analyse cladistique numérique et analyse de parcimonie ; l'exemple des Elephantidae. *Geobios* 19 (5): 587-600. http://dx.doi.org/10.1016/S0016-6995(86)80056-0

TASSY P. & DARLU P. 1987. — Les Elephantidae : nouveau regard sur les analyses de parcimonie. *Geobios* 20 (4): 487-494. http://dx.doi.org/10.1016/S0016-6995(87)80082-7

TOBIEN H. 1973. — On the evolution of mastodonts (Proboscidea, Mammalia). Part 1: the bunodont trilophodont groups. *Notizblatt des Hessischen Landesamtes für Bodenforschung zu Wiesbaden* 101: 202-276.

TOBIEN H. 1978. — On the evolution of Mastodonts (Proboscidea, Mammalia). Part 2: The bunodont tetralophodont Groups. *Geologisches Jahrbuch Hessen* 106: 159-208.

TOBIEN H., CHEN G.-F. & LI Y.-Q. 1988. — Mastodonts (Proboscidea, Mammalia) from the Late Neogene and Early Pleistocene of the People's Republic of China. Part II: historical account: the genera *Tetralophodon*, *Anancus*, *Stegotetrabelodon*, *Zygolophodon*, *Mammut*, *Stegolophodon*. *Mainzer geowissenschaftliche Mitteilungen* 17: 95-220.

WANG B.-Y. & QIU Z.-X. 2002. — A new species of *Platybelodon* (Gomphotheriidae, Proboscidea, Mammalia) from early Miocene of the Danghe area, Gansu, China. *Vertebrata PalAsiatica* 40 (4): 291-299.

WANG S.-Q. & YE J. 2015. — Paleobiological implications of new material of *Platybelodon danovi* from the Dingjiaergou Fauna, western China. *Historical Biology* 27 (8): 987-997. http://dx.doi.org/10.1080/08912963.2014.918967

WANG S.-Q., HE W., CHEN S.-Q. & DONG L.-P. 2013a. — A discussion of "*Mastodon*" *grandincisivus* based on new findings from the Late Miocene of the Linxia Basin, China., *in* REITNER J., YANG Q., WANG Y.-D. & REICH M. (eds), *Palaeobiology and Geobiology of Fossil Lagerstätten through Earth History*. Universitätsdrucke Göttingen, Göttingen: 176.

WANG S.-Q., HE W. & CHEN S.-Q. 2013b. — The gomphotheriid mammal *Platybelodon* from the middle Miocene of Linxia Basin, Gansu, China. *Acta Palaeontologica Polonica* 58: 221-240. http://dx.doi.org/10.4202/app.2011.0009

WANG S.-Q., LIU S.-P., XIE G.-P., LIU J., PENG T.-J. & HOU S.-K. 2013c. — *Gomphotherium wimani* from Wushan County, China and its implications for the Miocene stratigraphy of the Tianshui Area. *Vertebrata PalAsiatica* 51 (1): 71-84

WANG S.-Q., DENG T., TANG T., XIE G.-P., ZHANG Y.-G. & WANG D.-Q. 2015. — Evolution of *Protanancus* (Proboscidea, Mammalia) in East Asia. *Journal of Vertebrate Paleontology*. http://dx.doi.org/10.1080/02724634.2014.881830

YE J., WU W.-Y. & JIA H. 1990. — Reconstruction of the jaw-closing muscles of *Platybelodon tongxinensis* (Amebelodontidae, Proboscidea) and discussion of cranial evolution from long-jawed mastodont to short-jawed elephantid. *Vertebrata PalAsiatica* 28 (4): 284-295.

Submitted on 16 February 2015;
accepted on 13 July 2015;
published on 25 March 2016.

APPENDICES

APPENDIX 1. — Description of the characters used in the cladistic analysis. Most of the following characters are adopted or slightly modified from two previous studies: Tassy 1996 (T96) and Shoshani 1996 (S96). Others were selected specifically for this study.

0. Upper tusks: in lateral view. After T96:76 and S96:7. States: 0 = curving ventrally; 1 = relatively straight; 2 = curving dorsally.
1. Upper tusks: enamel band. After T96:72 and S96:10. States: 0 = present; 1 = absent.
2. Upper tusks: in anterior view. After S96:9. States: 0 = nearly parallel, 1 = divergent.
3. Lower tusks: absence. After T96:70 and S96:1. States: 0 = present; 1 = absent.
4. Lower tusks: shape of cross-section. After T96:74 and S96:15. States: 0 = flat, 1 = pyriform or sub-circular.
5. Lower tusks: thickness index (I = height/width). In the outgroup taxon *Phiomia* and most amebelodontines, lower tusks are moderately flattened, in contrast with very flattened lower tusks in *Platybelodon*; however, in *Gomphotherium* and *Tetralophodon*, lower tusks have sub-circular (pyriform) cross-section. States: 0 = I between 0.2 and 0.7, 1 = I smaller than 0.2, 2 = I larger than 0.7.
6. Lower tusks: inner structure. Tubular structure is present in some taxa, i.e. *Platybelodon* and *Konobelodon*; in contrast to the concentric laminar structures in the others. States: 0 = concentric laminae, 1 = dentinal tubules.
7. Lower tusks: exposed ratio (R = exposed lengh/symphyseal length). In the outgroup taxon *Phiomia*, exposed lengh of the lower tusks is very short relatively to symphyseal length; however, in some derived taxa (i.e. *Konobelodon robustus* n. sp. and *Stegotetrabelodon*), this length may be very large (i.e. larger than the symphyseal length). States: 0 = R smaller than 0.4, 1 = R between 0.4 and 1, 2 = R larger than 1.
8. Lower tusks: width index (I = width/exposed lengh). In the outgroup taxon *Phiomia* and most amebelodontines, lower tusks is moderately wide relatively to exposed lengh in contrast with very wide lower tusks in *Platybelodon*; however, in *Gomphotherium*, *Tetralophodon*, and *Stegotetrabelodon*, lower tusks is narrow. States: 0 = I between 0.3 and 0.6, 1 = I smaller than 0.3, 2 = I larger than 0.6.
9. Lower tusks: direction of the right and left one. States: 0 = parallel or slightly convergent; 1 = divergent.
10. Premolars: absence of premolars. After T96:86 and S96:27, modified. States: 0 = P2 or p2 present; 1 = P2 and p2 absent; 2 = P2, p2, and p3 absent; 3 = all the premolars absent.
11. Intermediate cheek teeth: number of loph(id)s. After T96:101-104 and S96:32, 33, 39, 40, modified. States: 0 = 3rd loph(id) not fully formed; 1 = typical trilophodont; 2 = 4th loph(id) formed at least on m2; 3 = 4 or more loph(id)s on m2.
12. Molars: compression of interloph(id)s. States: 0 = relatively open; 1 = relatively compressed; 2 = more compressed by dentinal plates like in elephantids.
13. Molars' pattern. After T96:106 and S96:60. States: 0 = bunodont; 1 = bunolophodont; 3 = dentinal plates.
14. Molars: posttrite central conules. After T96:113 and S96:55. States: 0 = no posttrite central conules; 1 = rudimentary posttrite central conules; 2 = completed posttrite trefoils.
15. m3: mesoconelets. After S96:59. States: 0 = mesoconelet smaller than main cusp; 1 = mesoconelet and main cusp of nearly equal size.
16. Molars: median sulcus. States: 0 = present; 1 = tending to be absent.
17. Molars: anancoidy. After T96:133. States: 0 = absent; 1 = pseudo-anancoidy; 2 = true anancoidy.
18. Cheek teeth: zygolophodonty, postrite half-loph(id)s and central conules crest-like. After T96:128 and S96:65. States: 0 = absent; 1 = present.
19. Cheek teeth: choerolophodonty, strong chevron with ptychodonty. After T96:131. States: 0 = present; 1 = absent.
20. Cheek teeth: stegodonty, pretrite mesoconelet fused with anterior central conule and staight loph(id). After T96:134. States: 0 = absent; 1 = present.
21. Cheek teeth: cementum. After T96:116 and S96:63. States: 0 = weak; 2 = heavy.
22. Cheek teeth: hypsodonty index. After S96:64.States: 0 = brachyodonty; 1 = meso-hypsodonty; 2 = true hypsodonty.
23. Cranium: distance between the temporal lines. After S96:73. States: 0 = sagittal crest present; 1 = temporal lines separated.
24. Cranium: in lateral view. After T96:37, modified. States: 0 = flat; 1 = moderately domed; 2 = strongly domed.
25. Maxilla: facial part. States: 0 = not elongated; 1 = anteriorly elongated; 2 = posteriorly retreated.
26. Nasal aperture: After T96:43 and S96:79. States: 0 = relatively narrow; 1 = perinasal fossa present.
27. Orbit: anterior border. After T96:30 and S96:83. States: 0 = situated above or posterior to M1; 1 = forward of M1.
28. Orbit: position. States: 0 = not close to the top of the cranium; 1 = close to the top of the cranium.
29. Basicanium: After T96:60, modified. States: 0 = not or slightly erected; 1 = moderately erected; 2 = strongly erected.
30. Palatine: spina nasalis posterior above choanae: After T96:31, S96:82. States: 0 = present; 1 = absent.
31. Infraorbital foramen: duplication on maxilla. After T96:33, S96:89. States: 0 = always present; 2 = sometimes present or absent.
32. Lacrymal foramen. After T96:42. States: 0 = present; 2 = absent.
33. Symphysis: elongation index (I = symphyseal length/length of cheek tooth row). After T96:48, 52 and S96:94, modified. States: I between 0.8 and 1.0, 1 = I smaller than 0.8, 2 = I between 1.0 and 1.3, 3 = larger than 1.3.

Appendix 1. — Continuation.

34. Symphysis: flattened. States: 0 = flattened; 1 = not flattened.
35. Symphysis: broadness index (I = symphyseal width/ length). In the outgroup taxon *Phiomia* and most amebelodontines, symphysis is moderately wide in contrast with very wide symphysis in *Platybelodon*; however, in other gomphotheres and elephantids, symphysis tusks is relatively narrow. States: 0 = I between 0.3 and 0.5; 1 = I larger than 0.5; 2 = I smaller than 0.3.
36. Symphysis: expansion index (I = maximal symphyseal width/ minimal symphyseal width). In the outgroup taxon *Phiomia* and some amebelodontines, anterior part of symphysis is moderately enlarged in contrast with acutely enlarged symphysis in *Platybelodon*; however, in other gomphotheres and elephantids, symphysis is only slightly enlarged or not enlarged. States: 0 = I between 1.25 and 2; 1 = I smaller than 1.25; 2 = I larger than 2.
37. Symphysis: anterior border: States: 0 = anteriorly oblique from both lateral sides to median axis; 1 = almost straight.
38. Symphysis: trough. After T96:67. States: 0 = shallow; 1 = deep.
39. Symphysis: distance between the posterior border and the cheek tooth row. After T96:50. States: 0 = close to each other, i.e. < *c.* 50 mm; 1 = remote, i.e. > *c.* 50 mm.
40. Symphysis: degree (D) of downward deflection. After T96:51, modified. In the outgroup taxon *Phiomia*, symphysis is almost straight relatively to the mandibular corpus; however, in some derived taxa (i.e. *Amebelodon*, *Konobelodon*, and *Stegotetrabelodon*), symphysis is acutely downward deflected. States: 0 = D smaller than 10°; 1 = D between 10° and 30°; 2 = D between 30° and 50°; 3 = D larger than 50°.
41. Ramus of mandible: degree (D) of posterior inclination. In primitive states (i.e. *Phiomia*), mandibular ramus is almostly perpendicular to the occlusal plan, in contrast with acutely posteriorly oblique ramus in *Platybelodon*; however, in elephantids, mandibular ramus is anteriorly oblique relatively to the occlusal plan. States: 0 = D between 90° and 100°; 1 = D between 100° and 120°; 2 = D larger than 120°; 3 = D smaller than 90°.
42. Corpus of mandible: lateral expansion. After T96:64. States: 0 = absent; 1 = present.

Appendix 2. — Cladistic data matrix of 43 characters scored for 16 taxa of the elephantiforms in the ingroup and *Phiomia* as the outgroup."?" in the matrix indicates that the character state is unknown for the taxon, and "–" indicates that the character is inapplicable for the taxon. Sources of data: *Phiomia*, Andrews (1906); *Gomphotherium*, Tassy (2013, 2014); *Archaeobelodon*, Tobien (1973); *Serbelodon*, Frick (1933); *Protanancus*, Wang *et al.* (2015); *Amebelodon*, Barbour (1927); *Konobelodon britti*, Lambert (1990); *Platybelodon*, Wang *et al.* (2013b); *Tetralophodon*, Mottl (1969) and Tobien (1978); *Paratetralophodon*, Tassy (1983b); *Anancus*, Tassy (1986); *Stegotetrabelodon*, Petrocchi (1943).

		1	2	3	4
	0	0	0	0	0
Phiomia	0000000000	0000000000	0000000000	0000000000	000
Zygolophodon	0000100010	1100000010	0001000101	0000100000	100
Choerolophodon	2101------	3100000001	0101010111	1100100110	210
Archaeobelodon	0000000000	1100000000	0001011101	??02001000	110
Serbelodon	0000000020	1100000000	0001???101	1100001000	100
Protanancus	0000000100	1100100100	0001011101	1102000001	110
Amebelodon	00?0000110	1100200100	000????10?	1103000001	200
Platybelodon	0110011020	2200100100	0101011100	1102012101	120
Konobelodon britti	0000001??0	1210200100	111?0??001	002101????	200
Konobelodon robustus n. sp.	0100001211	1210100100	0002101102	1112001001	200
Gomphotherium	0000120010	1100000000	0001001101	1102120001	010
Stegolophodon	1000120010	1211011000	1002101101	1100120000	100
Tetralophodon	0100120110	1210000000	0002101101	1102121001	200
Paratetralophodon	010???????	?210000000	0102121102	111???????	???
Anancus	1101------	2210000200	0002121102	11111----0	–31
Stegotetrabelodon	1100120210	1221011000	0112121102	1113121100	331
Elephas	2101------	3322011000	0122221102	11111----0	–31